International Multiphase Flow Technology Forum (IMFTF)

Friday, April 22nd , 2022

In situ measurement and imaging technique of particle separation in centrifugal fields by advanced wireless electrical resistance detector (aWERD)

Dr. Yosephus Ardean Kurnianto **PRAYITNO**[1,2]

Prof. Masahiro **TAKEI**[1]

[1]Graduate School of Science and Engineering, Chiba University

[2]Vocational College of Universitas Gadjah Mada

TAKEI Laboratory
武居　研究室
Laboratory on Multiphase Flow and Visualization

UNIVERSITAS GADJAH MADA

https://www.ihi.co.jp/separator/en/products/screw/hs-l.html

Where is Chiba Japan?

Tokyo (Narita) International Airport

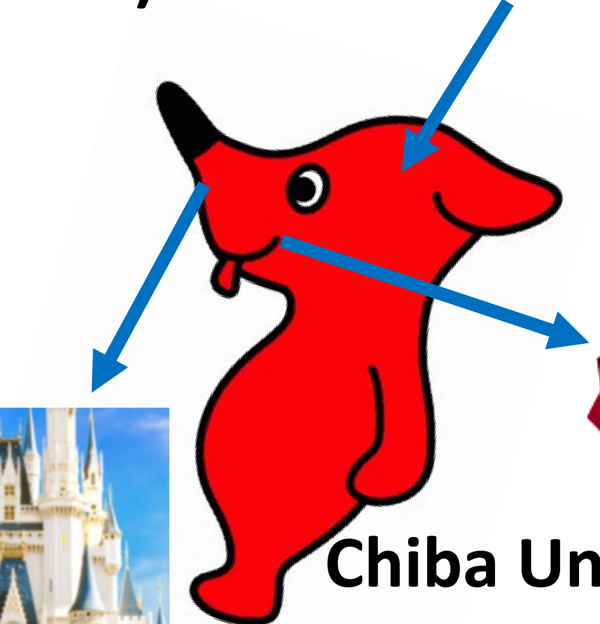

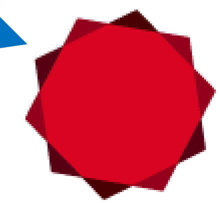

Chiba University

Chiba Kun

Tokyo Disneyland

OUTLINE

TAKEI Laboratory
武居　研究室
Laboratory on Multiphase Flow and Visualization

UNIVERSITAS GADJAH MADA

- ✓**Overview of Electrical Impedance Tomography[1] (5 min)**
- ✓ ***In situ* measurement on decanter centrifuge by Wireless Electrical Resistance Tomography (WERT) (40 min)**
- ✓ **Development of Lymphedema Monitor (10 min)**
- ✓ **Concluding Remarks and Questions (5 min)**

[1]J. Yao and M. Takei, Application of Process Tomography to Multiphase Flow Measurement in Industrial and Biomedical Fields -A Review, *IEEE Sensors Journal,* 17(24), 8196-8205 (2017)

Plant Group

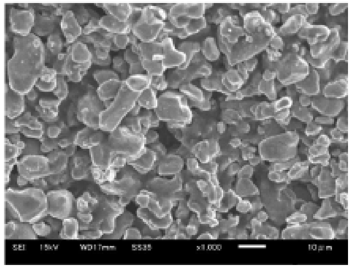

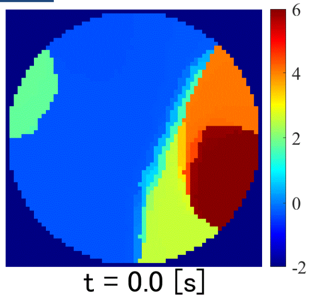

Lithium-ion battery slurry

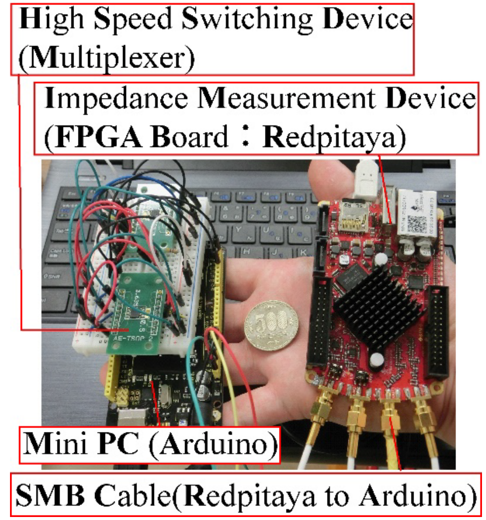

Bio Group

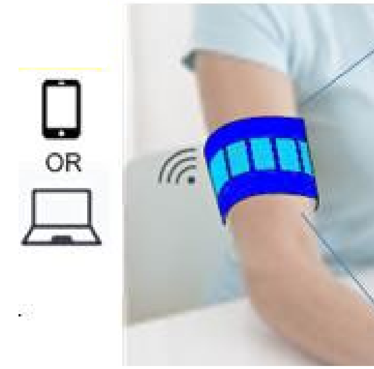

Lymphedema

Centrifuge

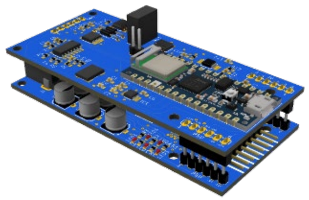

WERD/ WERT

Miniaturization

TAKEI Laboratory
武居　研究室
Laboratory on Multiphase Flow and Visualization

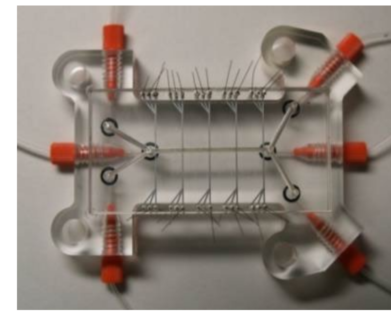

Micro-channel

Our Electrical Tomography & Applications

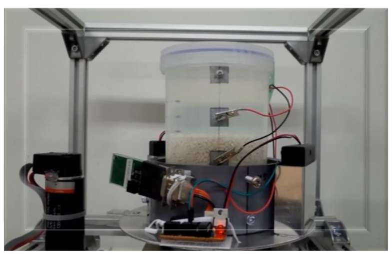

Wireless

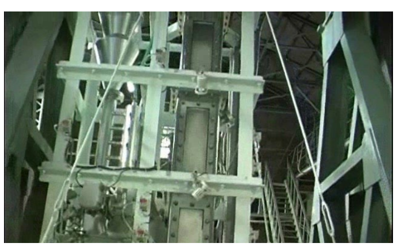

Energy Plant

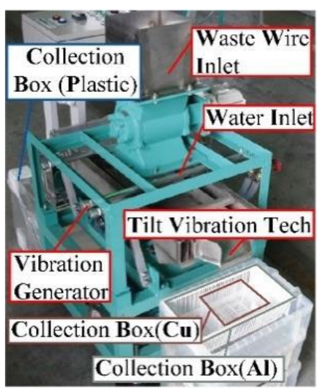

Vibration Separator

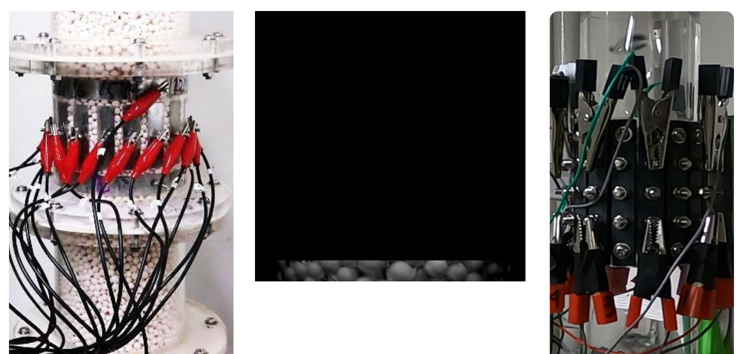

Chemical Reactor

Thrombosis

Provided by Prof. Nakamura

Overview of Electrical Impedance Tomography

https://youtu.be/nO6WWbqsin0

Basic Image Reconstruction

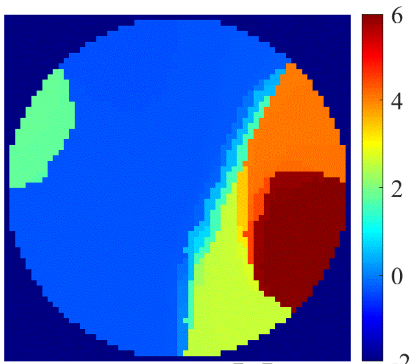

t = 0.0 [s]

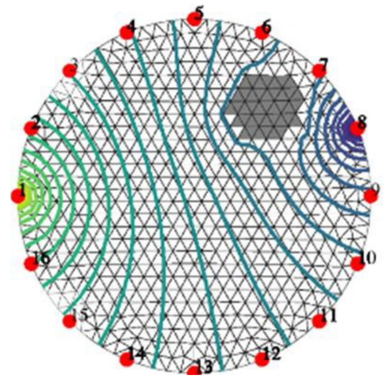

$$\Delta \mathbf{V} = \mathbf{J} \Delta \boldsymbol{\sigma}$$

$\Delta \mathbf{V}$: Measured relative voltage [-]

$\mathbf{J}$: Jacobian matrix [-]

$\Delta \boldsymbol{\sigma}$: relative conductivity [-]

Application: Prototype of Lymphedema Monitor

Wearable sensor

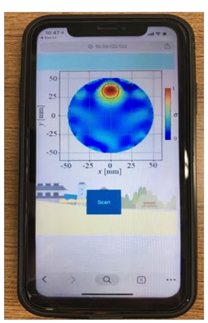

Display on Smartphone

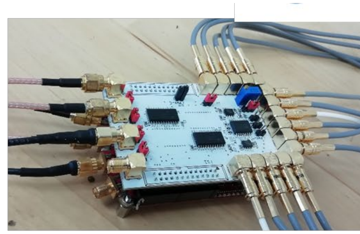

Handy measurement system

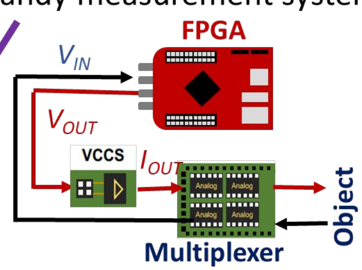

Cloud computing

LT Monitor

P. N. Darma and M. Takei, *IEEESensors Journal* (2020)

TAKEI Laboratory
武居　研究室
Laboratory on Multiphase Flow and Visualization

OUTLINE

TAKEI Laboratory
武居 研究室
Laboratory on Multiphase Flow and Visualization

UNIVERSITAS GADJAH MADA

✓Overview of Electrical Impedance Tomography[1] (5 min)

✓ ***In situ* measurement on industrial decanter by Wireless Electrical Resistance Tomography (WERT)[2-6] (40 min)**

✓ **Development of Lymphedema Monitor (10 min)**

✓ **Concluding Remarks and Questions (5 min)**

[2]Y. Atagi and M.Takei, real-time imaging of particles distribution in centrifugal particles-liquid two phase fields by wireless electrical resistance tomography (WERT) system, *IEEE Access*, Vol. 7. pp.12706 - 12713 (2019)

[3]K. Kimura, Y.A.K. Prayitno, and M. Takei, In situ particles deposition imaging in centrifugal fields by implemented SPH-DEM-ANN into linear sensor-type wireless electrical resistance tomography (lsWERT), *Powder Tech.,* Vol. 398, 117140 (2022)

[4]Z. Tong and M. Takei, real-time measurement of particle volume fraction in centrifugal fields by wireless electrical resistance detector (WERD), *Flow Meas. and Inst.,* 65, 90-97 (2018)

[5]Y. A. K. Prayitno and M. Takei, in-situ measurement of sludge thickness in high-centrifugal force by optimized particle resistance normalization for wireless electrical resistance detector (WERD), *Measurement Sci. & Tech.,* 32(3), 034001 (2020)

[6]Y.A.K. Prayitno and M. Takei, *In situ* measurement of hindered settling function in decanter centrifuge by periodic segmentation technique in wireless electrical resistance detector (*ps*WERD), *Advanced Powder Tech.,* 33(1), 103370 (2021)

Development of Wireless PT for Centrifuge[2]

TAKEI Laboratory
武居　研究室
Laboratory on Multiphase Flow and Visualization

WERT — **W**ireless **E**lectrical **R**esistance **T**omography

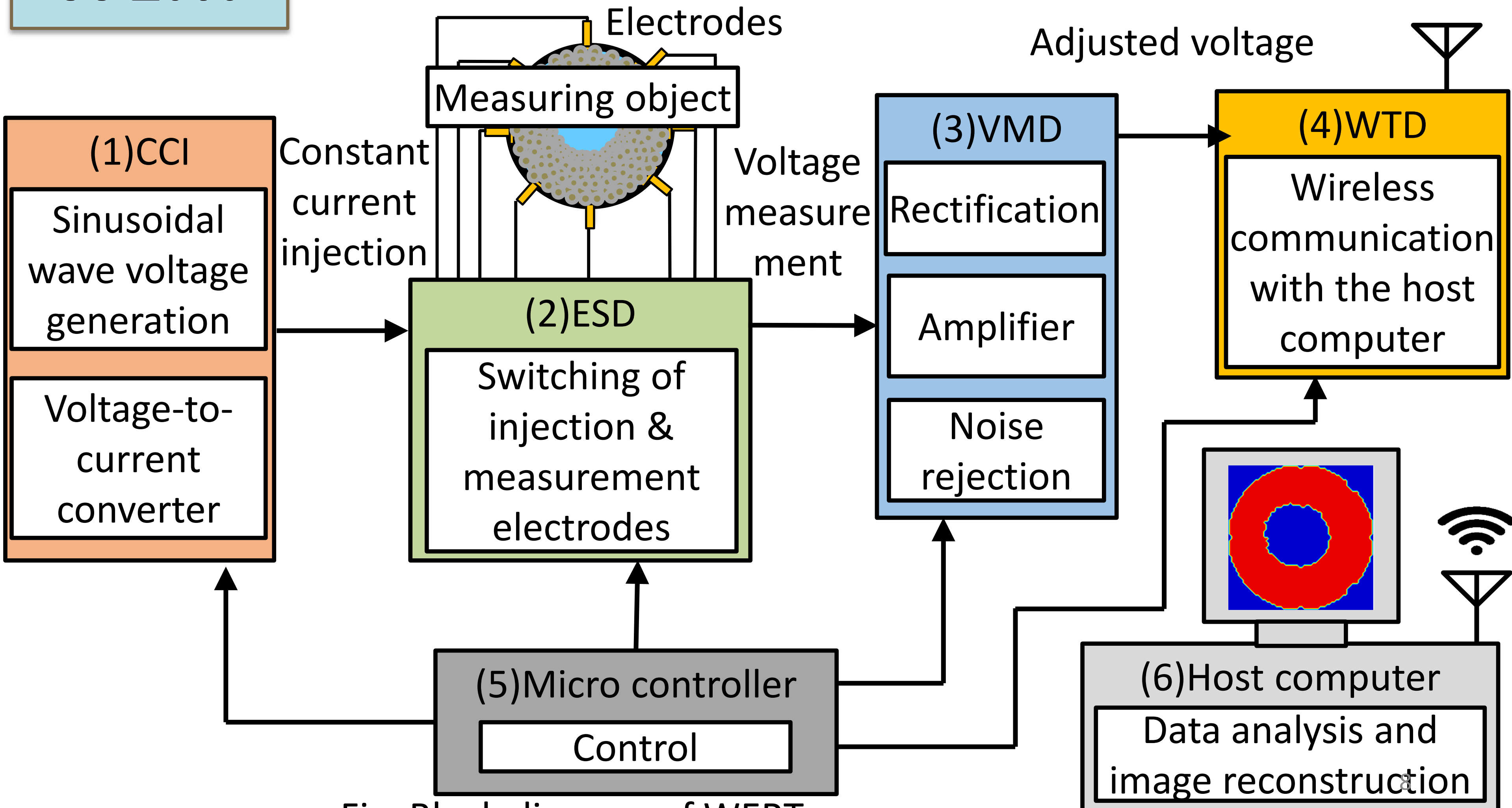

Fig. Block diagram of WERT

1) CCI : Constant-current injector
2) VMD : Voltage measurement device
3) ESD : Electrodes switching devices
4) WTD : Wireless transmission device

Experimental Setup of WERT in Lab Scale

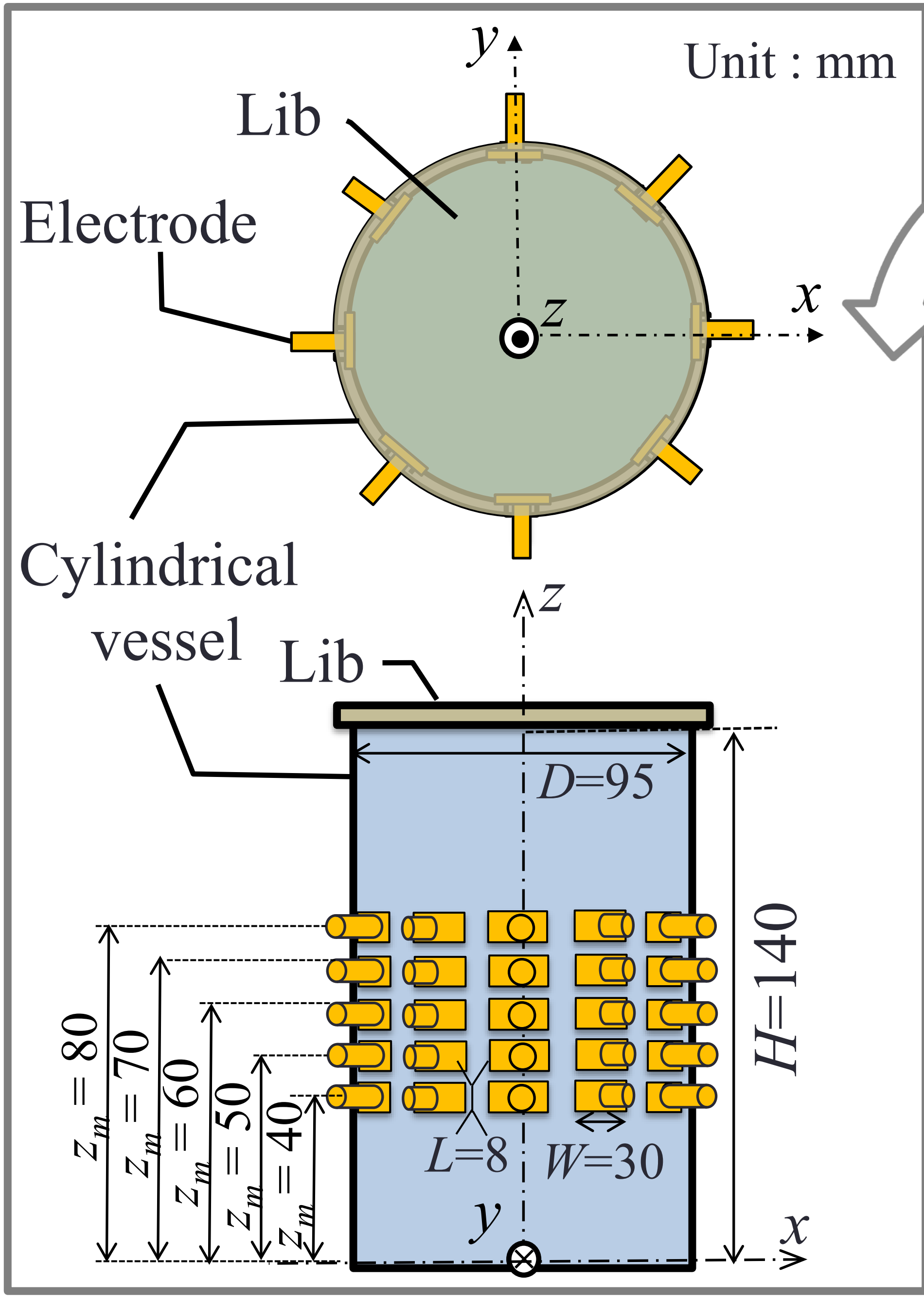

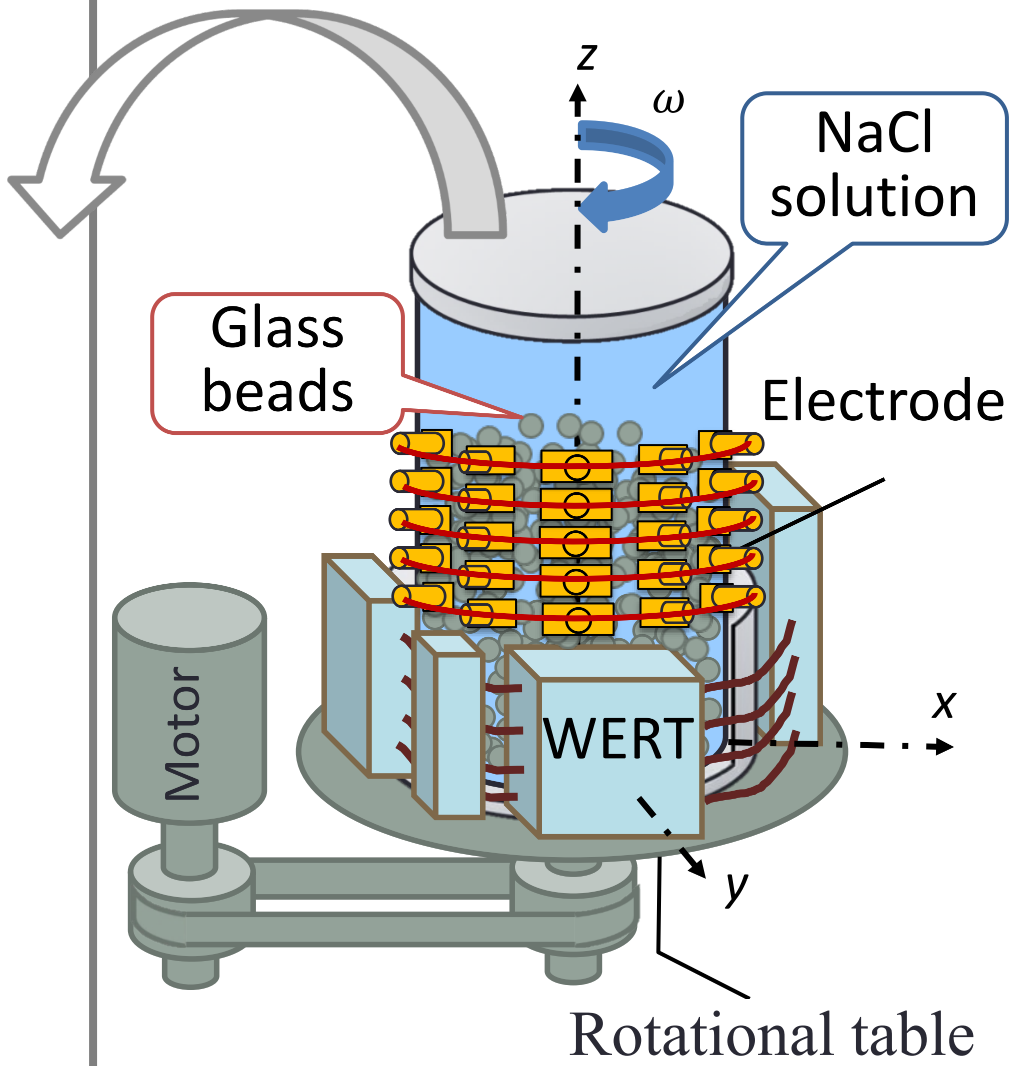

Fig. Diagram of experiment device

Experimental Conditions and Method

Conditions

- NaCl solution mass concentration ρ_w = 0.5wt%
- Glass beads particles size d = 2.0mm
- Glass beads filling rate S = 0.67
- Initial loading particles height h_p = 60mm
- Time resolution T_r = 0.5s/frame

Variable parameters

- Rotational speed ω = 170,230,290,350,410rpm
- Measurement position z_m = 40,50,60,70,80mm

Method

- Voltage U_{exp} measurement for 5 seconds at each conditions
- Calculate the conductivity distribution $\boldsymbol{\sigma}$ from the measured V_m
- Image reconstruction after converting $\boldsymbol{\sigma}$ into $\boldsymbol{\alpha}_\mathbf{p}$ by equation (1)

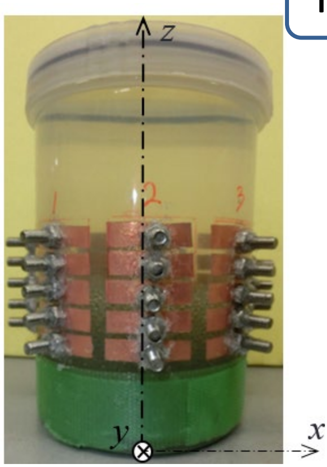

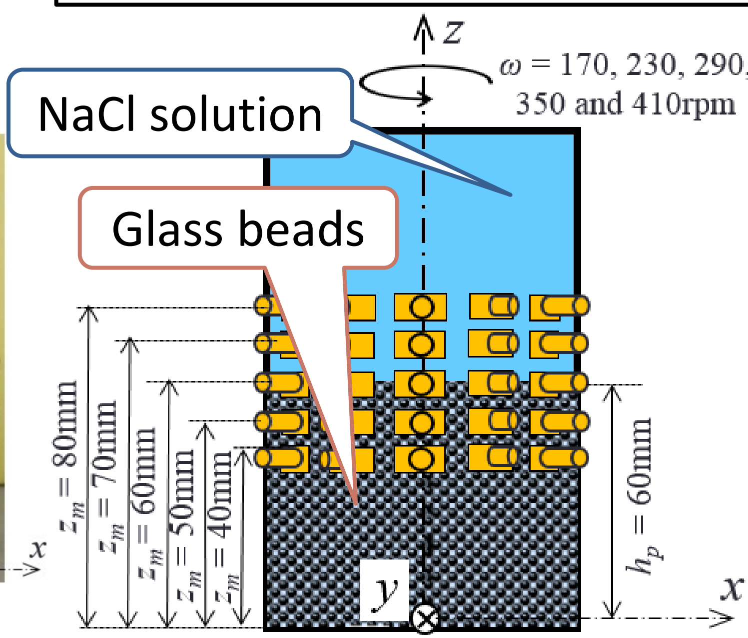

$$\alpha_p^{(i,j)} = \frac{(\sigma^{(i,j)} - \sigma_{\text{liquid}}^{(i,j)}) - \sigma_{\text{liquid}}}{\sigma_{\text{particles}} - \sigma_{\text{liquid}}} \cdots (1)$$

$\alpha_p^{(i,j)}$: Element of particle distribution $\boldsymbol{\alpha}_\mathbf{p}$

$\sigma^{(i,j)}$: Element of $\boldsymbol{\sigma}$

$\sigma_{\text{liquid}}^{(i,j)}$: Element of $\boldsymbol{\sigma}_{\textbf{liquid}}$

σ_{liquid} : $\boldsymbol{\sigma}$ in NaCl solution

$\sigma_{\text{particles}}$: $\boldsymbol{\sigma}$ in Close-packed glass beads + NaCl solution

3D Imaging of Particles Distribution α_p by WERT #1

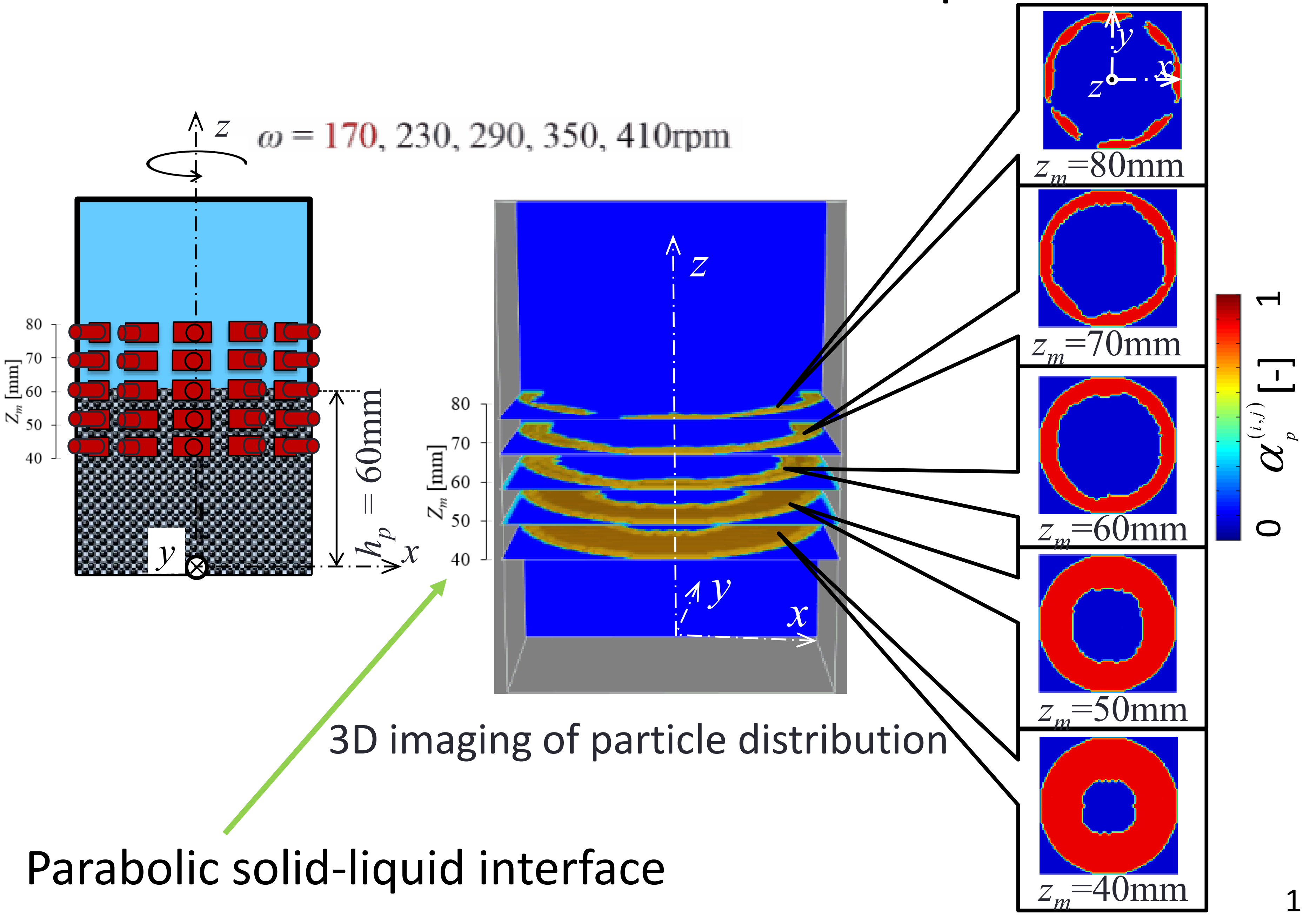

Parabolic solid-liquid interface

3D Imaging of Particles Distribution α_p by WERT #2

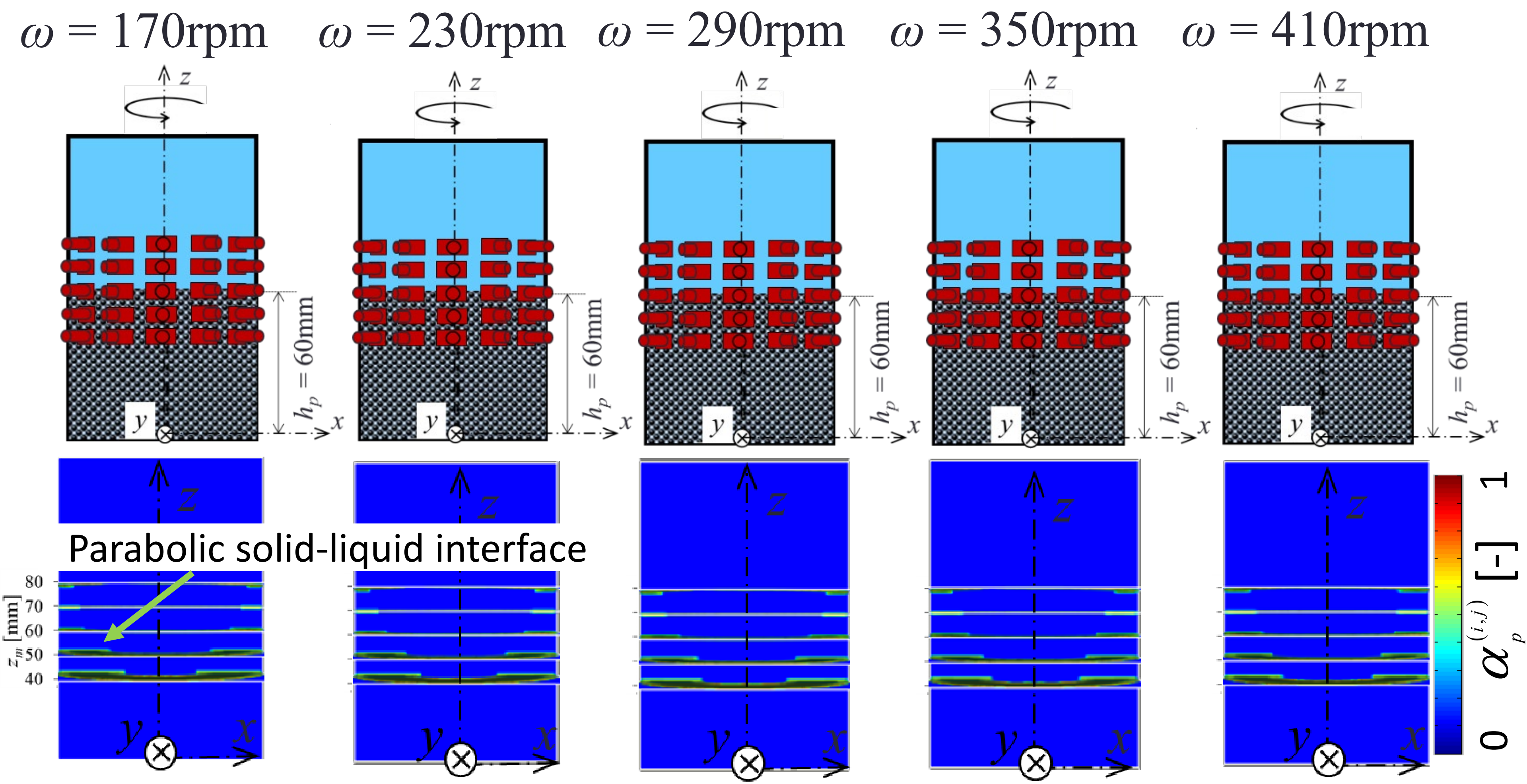

Parabolic solid-liquid interface becomes sharper as rotation velocity ω increase

TAKEI Laboratory
武居　研究室
Laboratory on Multiphase Flow and Visualization

Governing Equations of Simulation Model

Mass conservation equation

$$\frac{\partial \alpha_q}{\partial t} + \nabla \cdot (\alpha_q \mathbf{u}'_q) = 0$$

Simulation condition is the same as the experiment

Momentum conservation equation

$$\frac{\partial}{\partial t}(\alpha_q \rho_q \mathbf{u}'_q) + \nabla \cdot (\alpha_q \rho_q \mathbf{u}'_q \mathbf{u}'_q)$$

$$= -\alpha_q \nabla p + \nabla \cdot \overline{\overline{\tau}}_q + K_{ls} \Delta \mathbf{u}_{ls} + \mathbf{F}_{lift} + \mathbf{F}_{vm} + \alpha_q \rho_q [\mathbf{g} - \boldsymbol{\omega} \times (\boldsymbol{\omega} \times \mathbf{r}')]$$

$$+\rho_f \alpha_f (2\boldsymbol{\omega} \times \mathbf{u}_f + \frac{\mathrm{d}\boldsymbol{\omega}}{\mathrm{d}t} \times \mathbf{r})$$

Centrifugal force

Coriolis force

Euler force

Subscript *q* denotes either the liquid (*l*) or particle (*p*) phases

ρ: Density [kg/m^3]; α: Volume fraction [-]; $\alpha_p + \alpha_l = 1$

u ' : Velocity vector of fluid in moving reference frame;

p : Pressure shared by both phases[Pa]; $\overline{\overline{\tau}}$: Stress-strain tensor;

K_{ls}: Interphase momentum exchange coefficient between liquid and particle phase ;

$\Delta \mathbf{u}_{lp}$: Velocity difference between liquid and particle phase[m/s];

$\mathbf{F}_{lift}$: Lift force[N]; $\mathbf{F}_{vm}$: Virtual mass force[N];

$\boldsymbol{\omega}$: Angular velocity vector of the moving frame relative to stationary reference frame ;

r' : Position vector in the moving frame; *q*: Liquid phase or particle phase

Comparison between Experiment & Simulation

Condition	3Dimage	Simulation	z_m - $<\alpha_p>$ graph

ω=170rpm

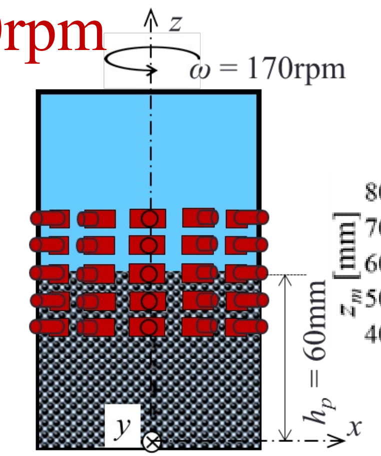

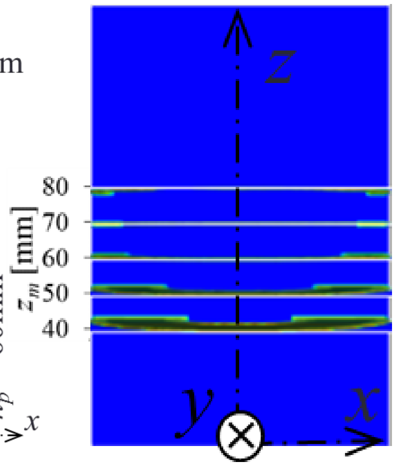

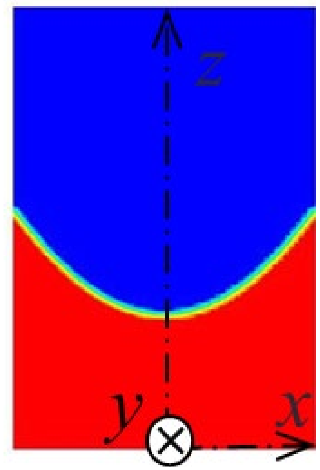

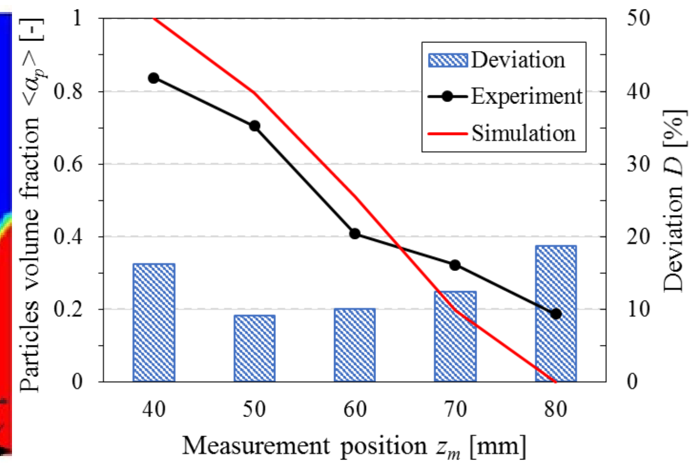

ω=230rpm

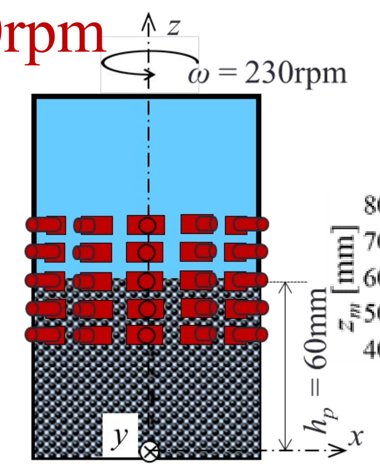

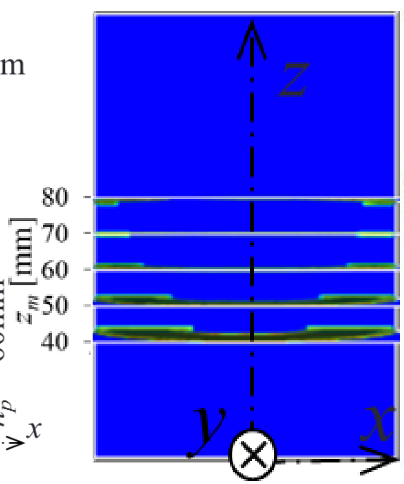

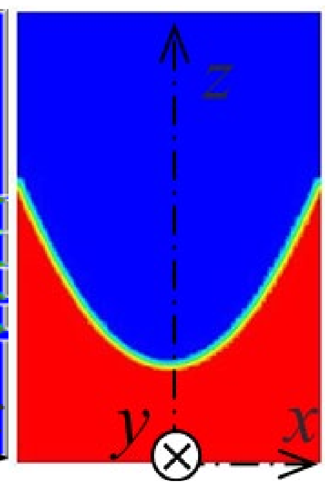

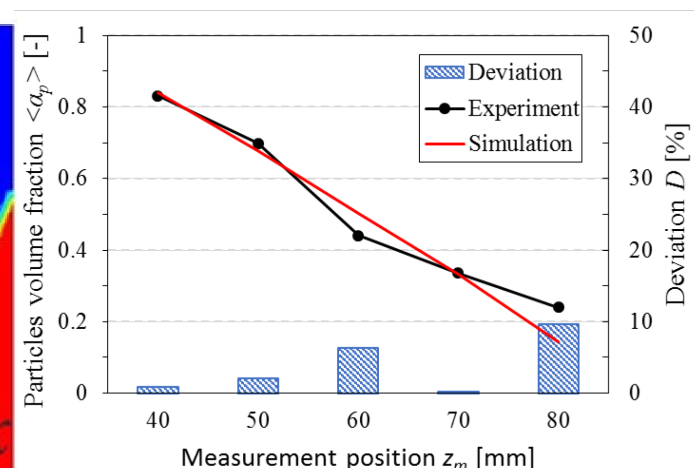

As shown in z_m-$<\alpha_p>$ graph, $<\alpha_p>$ by WERT presents the same variation trend with the numerical simulation

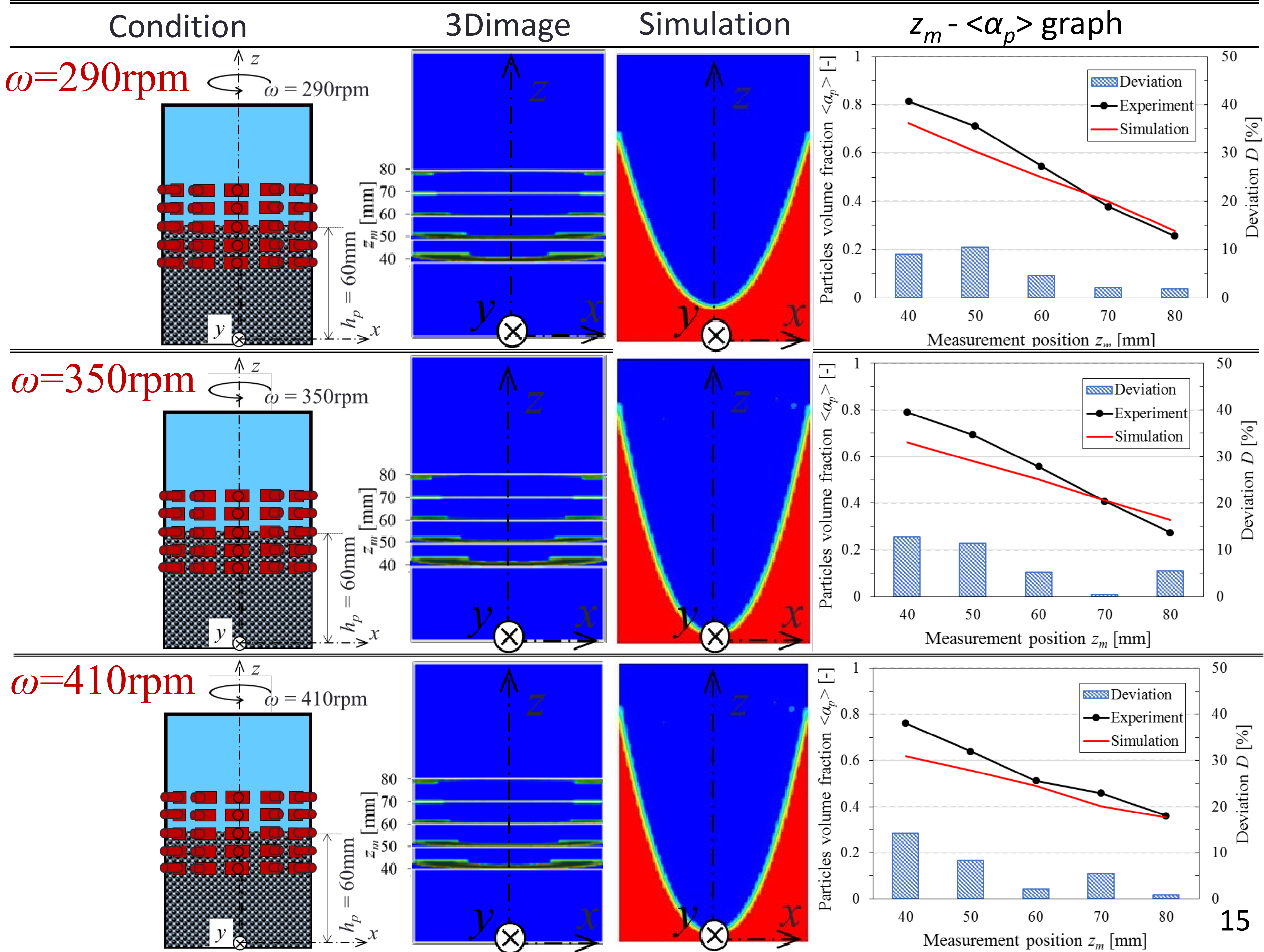

Condition
3Dimage
Simulation
zm - <αp> graph
ω=290rpm
ω = 290rpm
hp = 60mm
zm [mm]
80 70 60 50 40
Particles volume fraction <αp> [-]
Deviation D [%]
Measurement position zm [mm]
Deviation
Experiment
Simulation
ω=350rpm
ω = 350rpm
hp = 60mm
ω=410rpm
ω = 410rpm
hp = 60mm

OUTLINE

TAKEI Laboratory
武居　研究室
Laboratory on Multiphase Flow and Visualization

UNIVERSITAS GADJAH MADA

✓Overview of Electrical Impedance Tomography[1] (5 min)

✓ ***In situ* measurement on industrial decanter by Wireless Electrical Resistance Tomography (WERT)[2-6]** **(40 min)**

✓ **Development of Lymphedema Monitor** **(10 min)**

✓ **Concluding Remarks and Questions** **(5 min)**

[2]Y. Atagi and M.Takei, real-time imaging of particles distribution in centrifugal particles-liquid two phase fields by wireless electrical resistance tomography (WERT) system, *IEEE Access*, Vol. 7. pp.12706 - 12713 (2019)

[3]K. Kimura, Y.A.K. Prayitno, and M. Takei, In situ particles deposition imaging in centrifugal fields by implemented SPH-DEM-ANN into linear sensor-type wireless electrical resistance tomography (lsWERT), *Powder Tech.,* Vol. 398, 117140 *(*2022)

[4]Z. Tong and M. Takei, real-time measurement of particle volume fraction in centrifugal fields by wireless electrical resistance detector (WERD), *Flow Meas. and Inst.,* 65, 90-97 (2018)

[5]Y. A. K. Prayitno and M. Takei, in-situ measurement of sludge thickness in high-centrifugal force by optimized particle resistance normalization for wireless electrical resistance detector (WERD), *Measurement Sci. & Tech.,* 32(3), 034001 (2020)

[6]Y.A.K. Prayitno and M. Takei, *In situ* measurement of hindered settling function in decanter centrifuge by periodic segmentation technique in wireless electrical resistance detector (*ps*WERD), *Advanced Powder Tech.,* 33(1), 103370 (2021)

Overview of SPH-DEM-ANN coupled by *Is*WERT^3

Current issues

A lack of *in situ* image reconstruction technique for real-time particles-liquid separation in industrial decanter

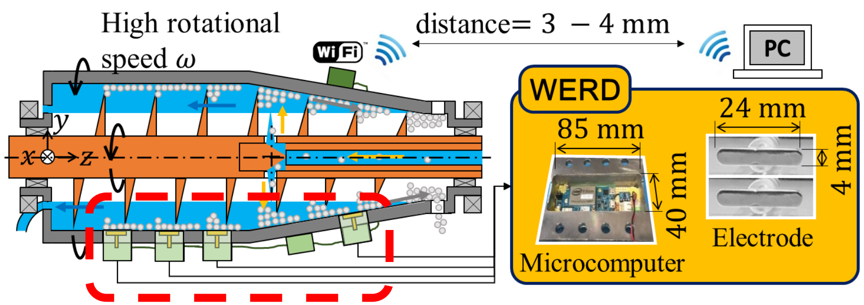

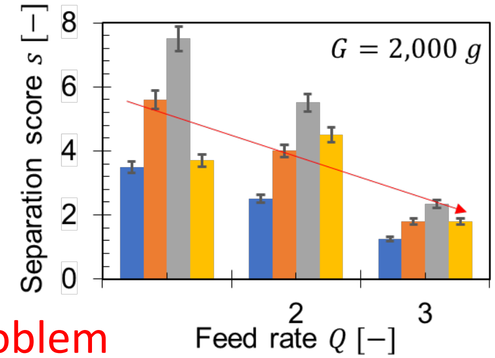

Pair-adjacent sensor-type WERD* problem

In situ particles deposition imaging in decanter problem

Technical problems

Conventional *Is*WERT problem

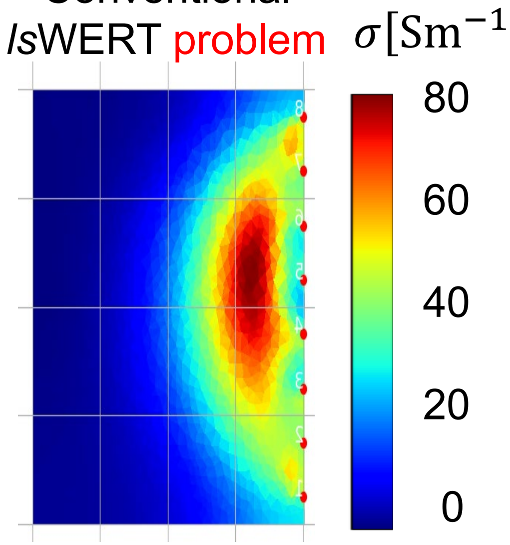

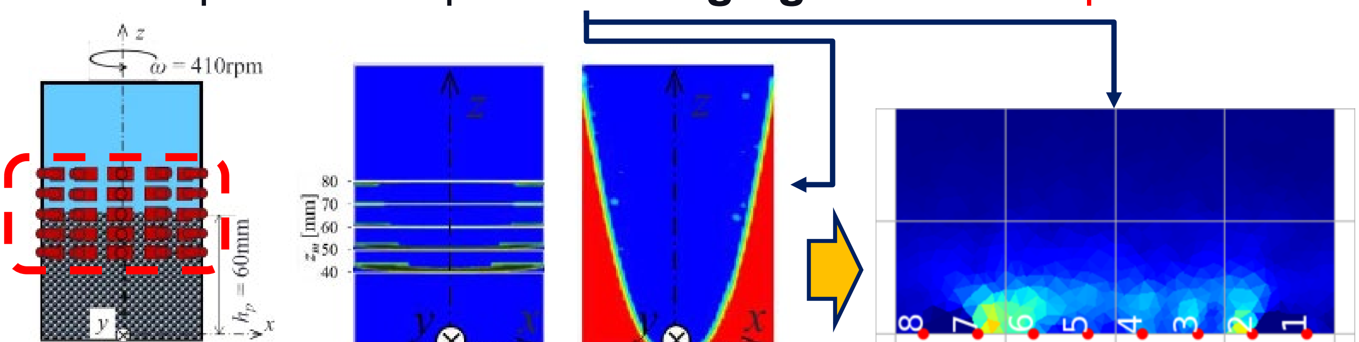

Circumferential sensor-type WERT**
problem

Linear sensor-type WERT
problem

Fig. WERT in various types

Research target

***In situ* particles deposition imaging** by **linear sensor**-type WERT coupled with **SPH-DEM-ANN**

*Y.A.K. Prayitno and M. Takei, *Meas. Sci. and Tech.*(2020)
**Y. Atagi and M. Takei, *IEEE Access* (2019)

TAKEI Laboratory
武居　研究室
Laboratory on Multiphase Flow and Visualization

Flowchart of SPH-DEM-ANN coupled by *ls*WERT[3]

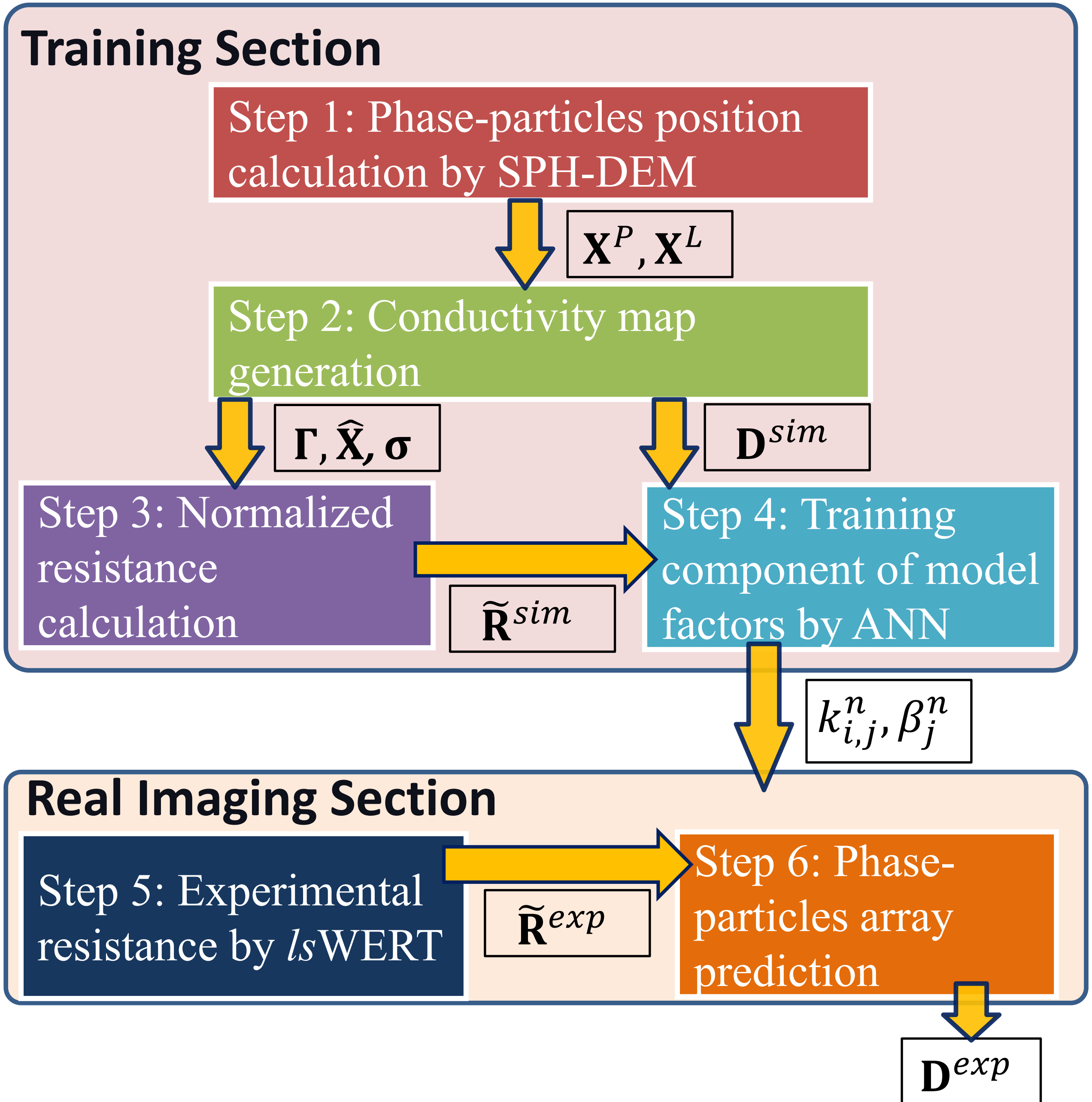

$\mathbf{X}^P$:Beads-particles position

$\mathbf{X}^L$:Liquid-particles position

$\boldsymbol{\Gamma}$:Elements array

$\widehat{\mathbf{X}}$:Node-particles array

$\boldsymbol{\sigma}$: Phase-particles conductivity array

$\mathbf{D}^{sim}$:Simulated material array

$\widetilde{\mathbf{R}}^{sim}$:Normalized simulated resistance array

$k_{i,j}^n$:Weight factor of ANN

β_j^n:Bias of ANN

$\widetilde{\mathbf{R}}^{exp}$:Normalized experimental resistance array

$\mathbf{D}^{exp}$:Experimental material array

Phase-particles position calculation by SPH-DEM (Step 1) #1

Constant values	
Density of liquid	ρ_L
Density of particle	ρ_P
Beads-particles diameter	d_p

Variables	
Beads-particles number	N_P
Liquid-particles number	N_L
Rotational speed	ω

Step 1: Phase-particles position calculation by SPH-DEM

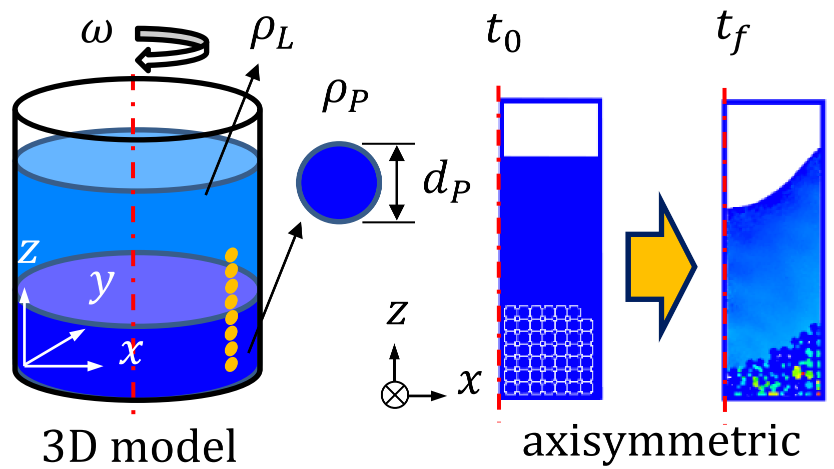

Fig. SPH-DEM simulation model

Calculated of phase-particles position

Beads-particles position:

$$\mathbf{X}^P = \left[(x_1^P, z_1^P), \dots (x_n^P, z_n^P), \dots (x_{N_P}^P, z_{N_P}^P)\right]^T \in \mathbb{R}^{N_P}$$

Liquid-particles position:

$$\mathbf{X}^L = \left[(x_1^L, z_1^L), \dots (x_n^L, z_n^L), \dots (x_{N_L}^L, z_{N_L}^L)\right]^T \in \mathbb{R}^{N_L}$$

Phase-particles position calculation by SPH-DEM (Step 1) #2

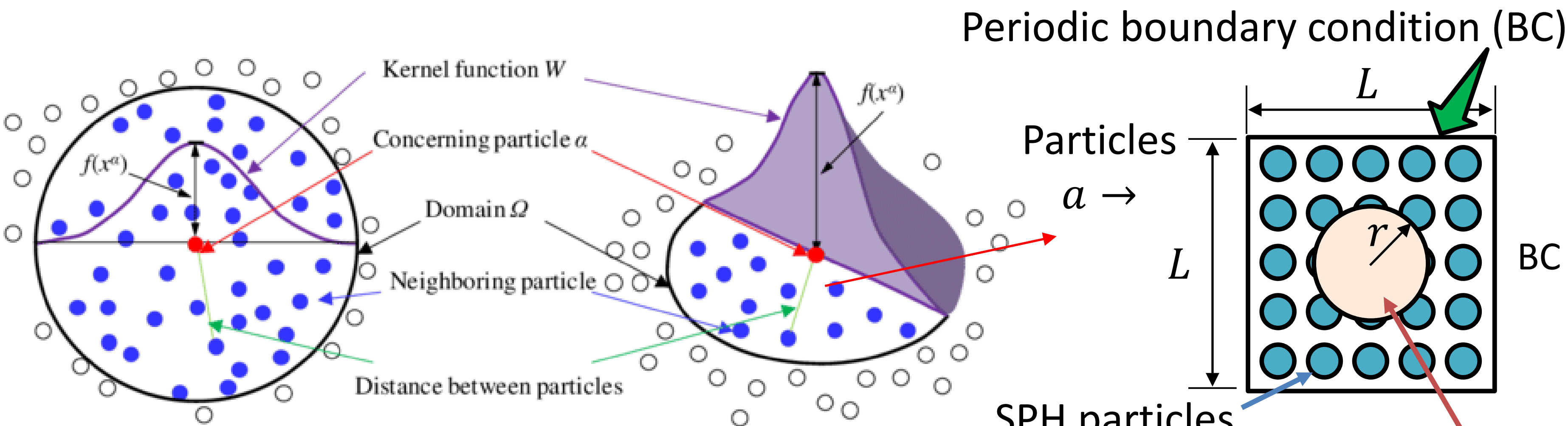

Fig. SPH-DEM overview

Calculation of the radius of neighbour liquid-particles a and b for liquid-particles position in axisymmetric centrifugal fields

$$\rho_a = \sum_b m_b W_{ab}(q) \quad (1)$$

$$W_{ab}(q) \begin{cases} \frac{10}{7\pi h^2}\left(1 - \frac{3}{2}q^2\left(1 - \frac{q}{2}\right)\right) & 0 \leq q \leq 1 \\ \frac{5}{14\pi h^2}(2-q)^3 & 1 \leq q \leq 2 \\ 0 & 2 \leq q \end{cases} \quad (2)$$

$\rho_a[\mathrm{kgm}^{-3}]$: density of particles a

$m_a[\mathrm{kg}]$: mass of particles a

$W_{ab}[-]$: Kernel function for particles $a \rightarrow b$

$q[-]$: dimensionless length

$h[\mathrm{mm}]$: smoothing length

Phase-particles position calculation by SPH-DEM (Step 1) #3

$$\frac{\nabla P_a}{\rho_a} = \sum_b m_b \frac{P_b}{\rho_b^2} \nabla W_{ab} + \sum_b m_b \frac{P_a}{\rho_a^2} \nabla W_{ab} \qquad (3)$$

Pressure difference $P_b - P_a$ by centrifugal force $\mathbf{F}_{a\leftarrow b}^{c}$ as,

$$\mathbf{F}_{a\leftarrow b}^{c} = -m_a m_b \left(\frac{P}{\rho^2}\right) \nabla W_{ab} \qquad (4)$$

Momentum equation for liquid-particles influenced by $\mathbf{F}_{a\leftarrow b}^{c}$

$$\frac{\mathrm{d}\mathbf{v}_\mathrm{a}}{\mathrm{d}t} = -\sum_b m_b \left(\frac{P_b}{\rho_b^2} + \frac{P_a}{\rho_a^2} + \Pi_{ab}\right) \nabla W_{ab} \qquad (5)$$

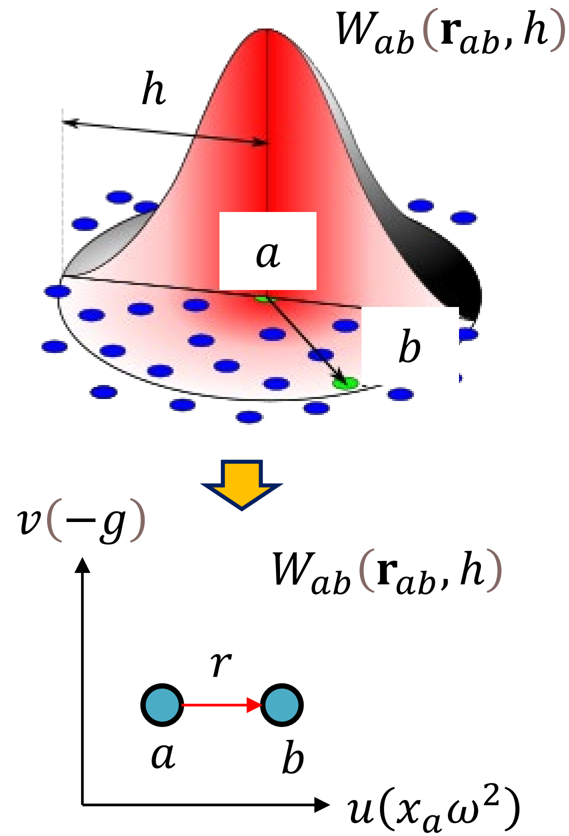

Fig. Phase-particles position mechanism

P_a[Pa]: Pressure of particles a

P_b[Pa]: Pressure of particles b

$\Pi_{ab}[\mathrm{ms}^{-1}]$: velocity difference in artificial velocity

TAKEI Laboratory
武居 研究室
Laboratory on Multiphase Flow and Visualization

Phase-particles position calculation by SPH-DEM (Step 1) #4

Solving liquid-particles position in axisymmetric centrifugal fields

$$\Pi_{ab} = \begin{cases} \dfrac{-\alpha \bar{c}_{ab} \mu_{ab}}{\bar{\rho}_{ab}} & \mathbf{v}_{ab} \cdot \mathbf{r}_{ab} < 0 \\ 0 & \mathbf{v}_{ab} \cdot \mathbf{r}_{ab} > 0 \end{cases} \quad (6)$$

$$\mu_{ab} = \frac{h \mathbf{v}_{ab} \cdot \mathbf{r}_{ab}}{\mathbf{r}_{ab}^2 + \eta^2} \quad (7)$$

$$\bar{c}_{ab} = \frac{c_a + c_b}{2} \quad (8)$$

$$\bar{\rho}_{ab} = \frac{\rho s_a + \rho s_b}{2} \quad (9)$$

Smoothing prevention under the case of $\mathbf{r}_{ab} < 0.1h \rightarrow \eta^2 = 0.01h^2$

$\alpha[\mathrm{mm}]$: radius of shear and bulk viscosity

$\bar{c}_{ab}[\mathrm{ms}^{-1}]$: mean sound speed of liquid-particles

$\mu_{ab}[\mathrm{Pas}]$: smoothed viscosity of liquid-particles

$\bar{\rho}_{ab}[\mathrm{kgm}^{-3}]$: mean density of liquid-particles

$\eta[-]$: dimensionless viscous term to prevent singularities

Phase-particles position calculation by SPH-DEM (Step 1) #5

Solving particles-phase flow in SPH-DEM for bead-particles velocity $\mathbf{v}_P$

$$\frac{\mathrm{d}\mathbf{v}_P}{\mathrm{d}t} = \sum_L m_L \frac{V_P}{\rho_L} \frac{2P_P}{\rho_L^2} \nabla W_{PL} \qquad (10)$$

$$\nabla W_{PL} = \nabla W(\mathbf{r}_P - \mathbf{r}_L, h)$$

Solving Eq.(1)-(10), phase-particles position:

$$\mathbf{x}_n^P = [(x_n^P, z_n^P)]^T \text{ and } \mathbf{x}_n^L = [(x_n^L, z_n^L)]^T \qquad (11)$$

$$\mathbf{X}^P = \left[\mathbf{x}_1^P \ldots \mathbf{x}_n^P, \ldots \mathbf{x}_{N_p}^P\right]^T \in \mathbb{R}^{N_P} \qquad (12)$$

$$\mathbf{X}^L = \left[\mathbf{x}_1^L \ldots \mathbf{x}_n^L, \ldots \mathbf{x}_{N_p}^L\right]^T \in \mathbb{R}^{N_L} \qquad (13)$$

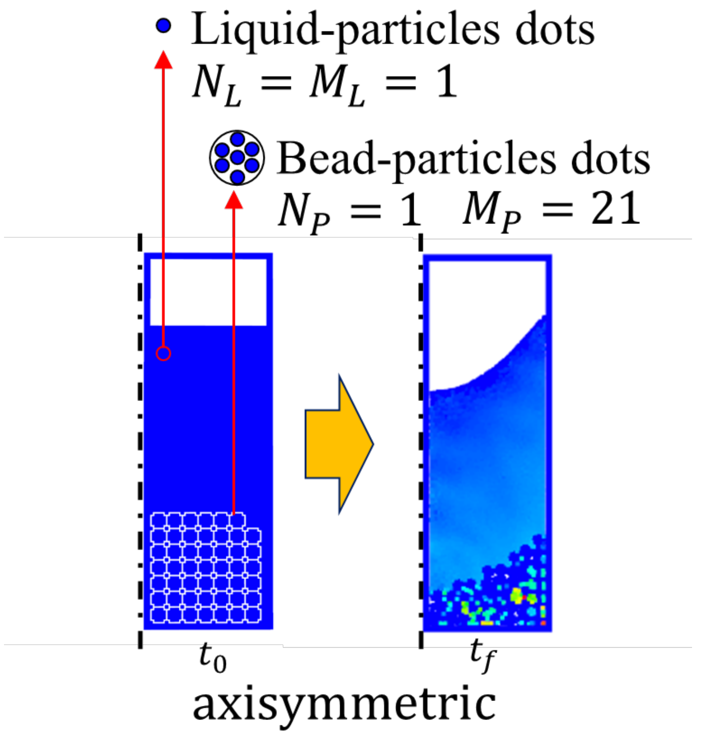

Fig. SPH-DEM simulation model

m_P[kg]: mass of bead-particles

m_L[kg]: mass of liquid-particles

P_P[Pa]: Pressure of bead-particles

P_L[Pa]: Pressure of liquid-particles

ρ_P[kgm^{-3}]: density of bead-particles

ρ_L[kgm^{-3}]: summation density of liquid-particles

V_P[m^3]: Volume of bead-particles relative to bead-particles number M_P

$\mathbf{X}^P$[mm]: position array of bead-particles

$\mathbf{X}^L$[mm]: position array of liquid-particles

Conductivity map generation (Step 2) #1

Step 1: Phase-particles position calculation by SPH-DEM

$\mathbf{X}^P, \mathbf{X}^L$

Step 2: Conductivity map generation

Coincided phase-particles position array:

$$\hat{\mathbf{x}}_n = \left[\left(\hat{x}_{\lambda_n}, \hat{z}_{\lambda_n}\right)\right]^T \in \mathbb{R}^2 \begin{cases} \hat{\mathbf{x}}_n^P \\ \hat{\mathbf{x}}_n^L \end{cases}$$

Triangle mesh array:

$$\boldsymbol{\gamma}_n = \left[\gamma_{\lambda_1}, \gamma_{\lambda_2}, \gamma_{\lambda_3}\right] \in \mathbb{R}^3 \begin{cases} \boldsymbol{\gamma}_n^P \\ \boldsymbol{\gamma}_n^L \end{cases}$$

Constant values

Conductivity of bead-particles	σ_n^P
Conductivity of liquid-particles	σ_n^L
Conductivity of air-particles	σ_n^0

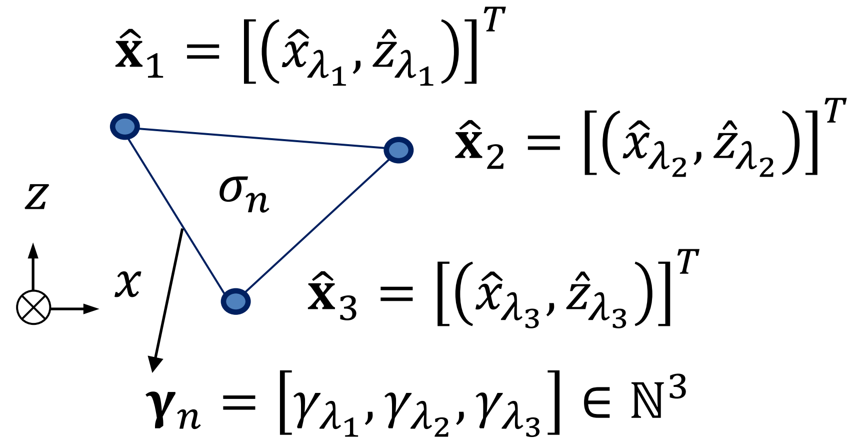

$\boldsymbol{\Gamma}, \hat{\mathbf{X}}, \boldsymbol{\sigma}$

Elements array:

$$\boldsymbol{\Gamma} = \left[\boldsymbol{\gamma}_1, \ldots \boldsymbol{\gamma}_n, \ldots \boldsymbol{\gamma}_{N_\gamma}\right]^T \in \mathbb{R}^{N_\gamma}$$

Node-particles array:

$$\hat{\mathbf{X}} = \left[\hat{\mathbf{x}}_1, \ldots \hat{\mathbf{x}}_n, \ldots \hat{\mathbf{x}}_{N_\lambda}\right]^T \in \mathbb{R}^{N_\lambda}$$

Phase-particles conductivity array:

$$\boldsymbol{\sigma} = \left[\sigma_1, \ldots \sigma_n, \ldots \sigma_{N_\gamma}\right]^T \in \mathbb{R}^{N_\gamma}$$

$\mathbf{D}^{sim}$

Simulated material array:

$$\mathbf{D}^{sim} = \left[D_1^{sim}, \ldots D_n^{sim}, \ldots D_{N_\gamma}^{sim}\right] \in \mathbb{R}^{N_\gamma}$$

Step 3: Normalized resistance calculation

Step 4: Training component of model factors by ANN

Conductivity map generation (Step 2) #2

2-1) Extraction step of phase-particles dot

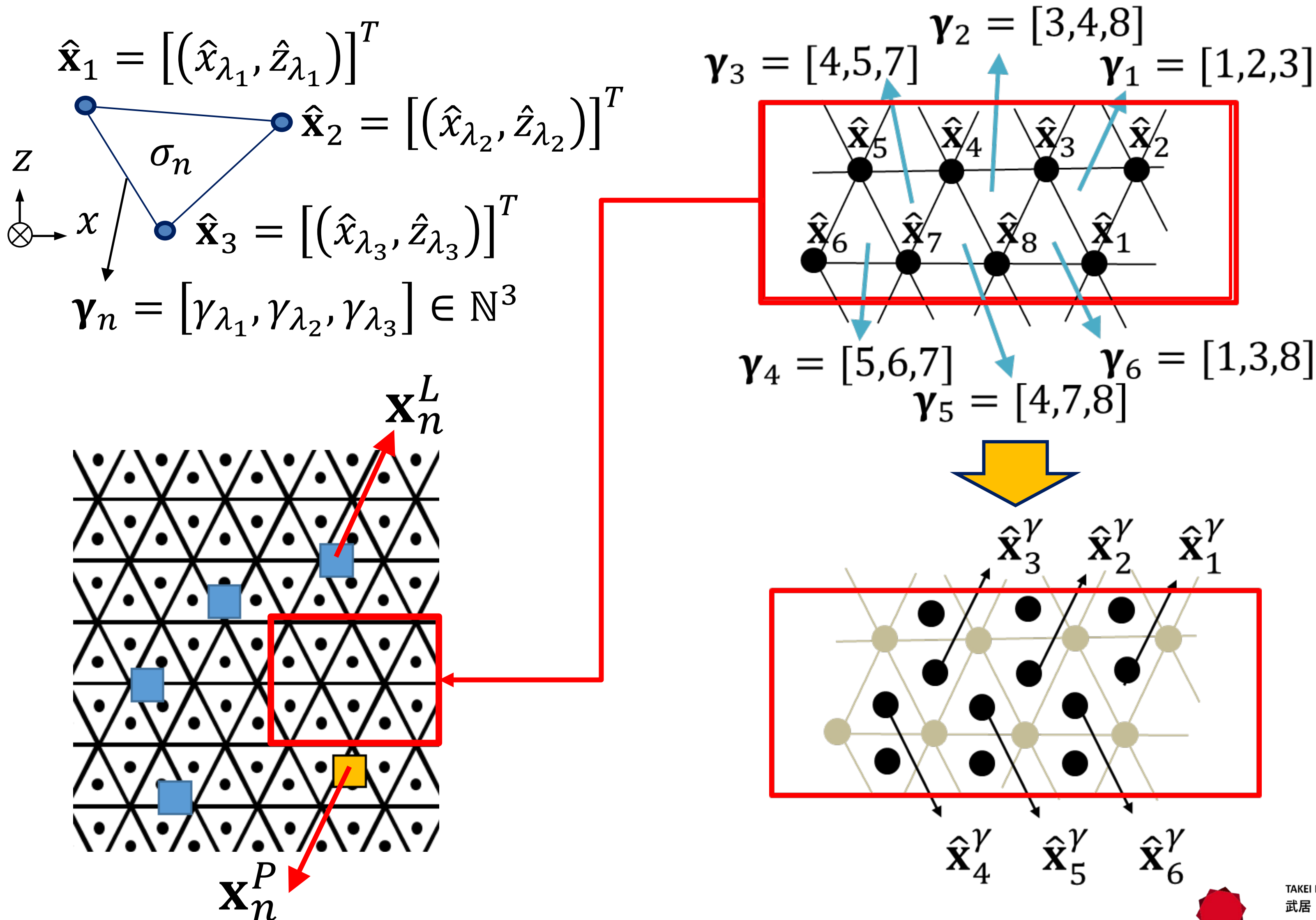

Fig. Schematic of extraction step

Conductivity map generation (Step 2) #3

2-2) Conversion step of phase-particles dots → **2-3) Generation step of conductivity map**

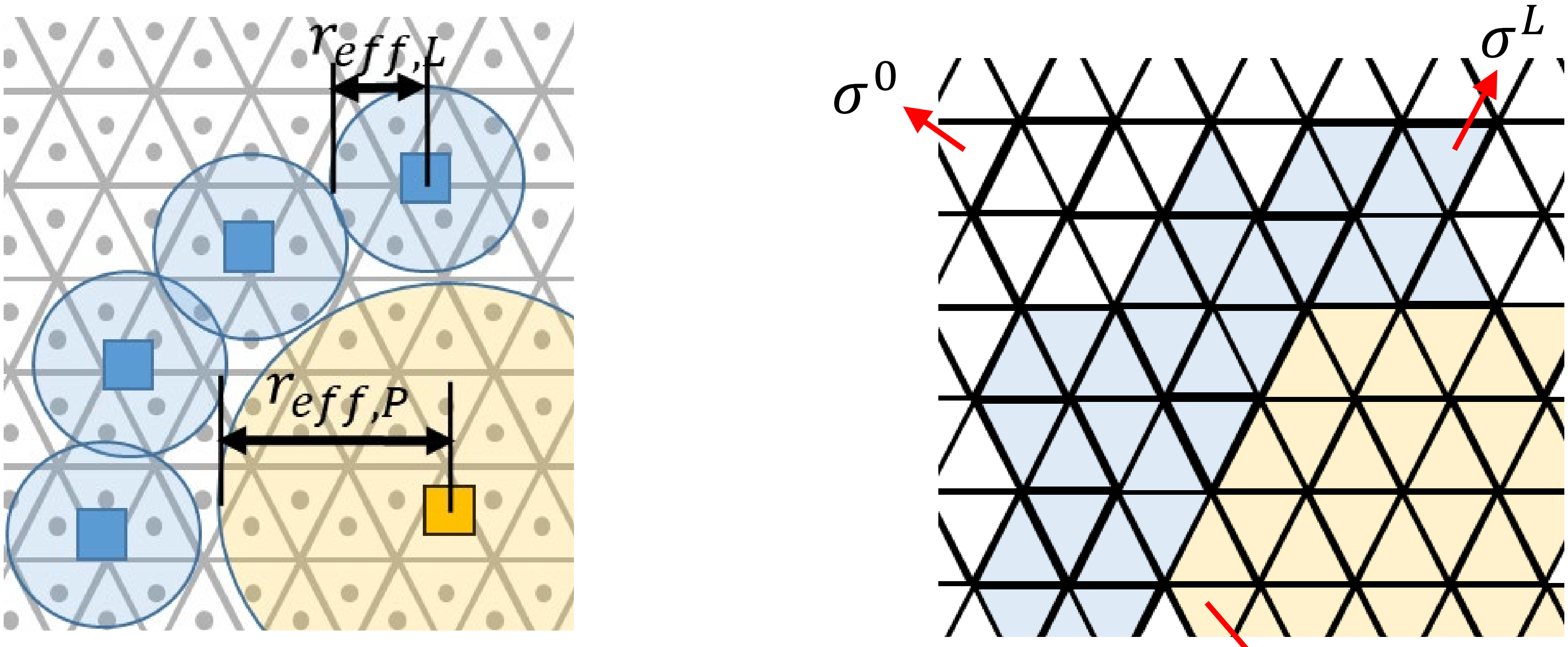

Fig. Schematic of conversion and generation steps

- r_{eff} solved under closed-pack conditions as $d/\sqrt{3}$

$$\sigma_n \begin{cases} \sigma_n^P & \text{If } \min\left(\left\|\hat{\mathbf{x}}_n^{\gamma} - \mathbf{X}^P\right\|\right) < r_{eff,P} \\ \sigma_n^L & \text{Else if } \min\left(\left\|\hat{\mathbf{x}}_n^{\gamma} - \mathbf{X}^L\right\|\right) < r_{eff,L} \\ \sigma_n^0 & \text{Else} \end{cases} \quad (14)$$

$$D_n^{sim} \begin{cases} 0 & \text{for } \sigma_n^0 \text{ represented air-phase} \\ 1 & \text{for } \sigma_n^L \text{ represented liq-phase} \\ 2 & \text{for } \sigma_n^P \text{ represented par-phase} \end{cases} \quad (15)$$

Normalized resistance calculation (Step 3)

Step 2: Conductivity map generation

$\mathbf{\Gamma}, \hat{\mathbf{X}}, \boldsymbol{\sigma}$

Step 3: Normalized resistance calculation

Simulated resistance array:

$$\mathbf{R}^{sim} = \left[R_1^{sim}, \dots R_n^{sim}, \dots R_{N_{sw}}^{sim}\right]^T \in \mathbb{R}^{N_{sw}}$$

Reference simulated resistance array:

$$\breve{\mathbf{R}}^{sim} = \left[\breve{R}_1^{sim}, \dots \breve{R}_n^{sim}, \dots \breve{R}_{N_{sw}}^{sim}\right]^T \in \mathbb{R}^{N_{sw}}$$

$\widetilde{\mathbf{R}}^{sim}$

Normalized simulated resistance array:

$$\widetilde{\mathbf{R}}^{sim} = \mathbf{R}^{sim} / \breve{\mathbf{R}}^{sim} \in \mathbb{R}^{N_{sw}}$$

$$\widetilde{\mathbf{R}}^{sim} = \left[R_1^{sim}, \dots R_{n_{sw}}^{sim}, \dots R_{N_{sw}}^{sim}\right]^T \in \mathbb{R}^{N_{sw}}$$

Step 4: Training component of model factors by ANN

Constant values	
Number of switching electrode pattern	N_{sw}
1st electrode height	Z_1^{el}
Electrode distance	ΔZ^{el}

Governing Equations:

$$\nabla \cdot \left(\sigma_{n_e} \nabla \phi_{n_e}\right) = 0 \qquad (16)$$

$$\sigma \frac{\partial \phi}{\partial \boldsymbol{\xi}} = \mathrm{J}_{n_{el}} \qquad (17)$$

$$R_{n_{sw}}^{sim} = \frac{\phi_{n_{el(HP)}} - \phi_{n_{el(LP)}}}{I_c} \qquad (18)$$

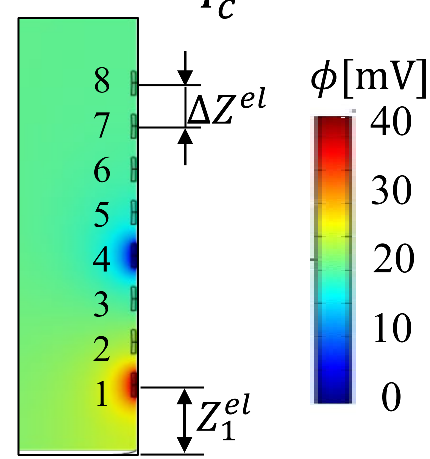

Fig. Simulation model

Model factors training (Step 4)

Step 3: Normalized resistance calculation

$\widetilde{\mathbf{R}}^{sim}$

Step 2: Conductivity map generation

$\mathbf{D}^{sim}$

Step 4: Training component of model factors by ANN

1st output neurons:

$$e_j^1 = f_h\left(\sum_{i=1}^{N_{sw}} k_{i,j}^1 \cdot \tilde{R}_i + \beta_j^1\right)$$

2nd output neuorns:

$$e_j^2 = f_o\left(\sum_{i=1}^{N_h} k_{i,j}^2 \cdot e_j^1 + \beta_j^2\right)$$

$k_{i,j}^n, \beta_j^n$

Trained model factors	
Weight factor	$k_{i,j}^n$
Bias	β_j^n

Step 6: Phase-particles array prediction

Constant values	
Number of hidden layer nodes	N_h
Hidden layer activation function (ReLu)	f_h
Number of output layer nodes	N_o
Hidden layer activation function (SoftMax)	f_o

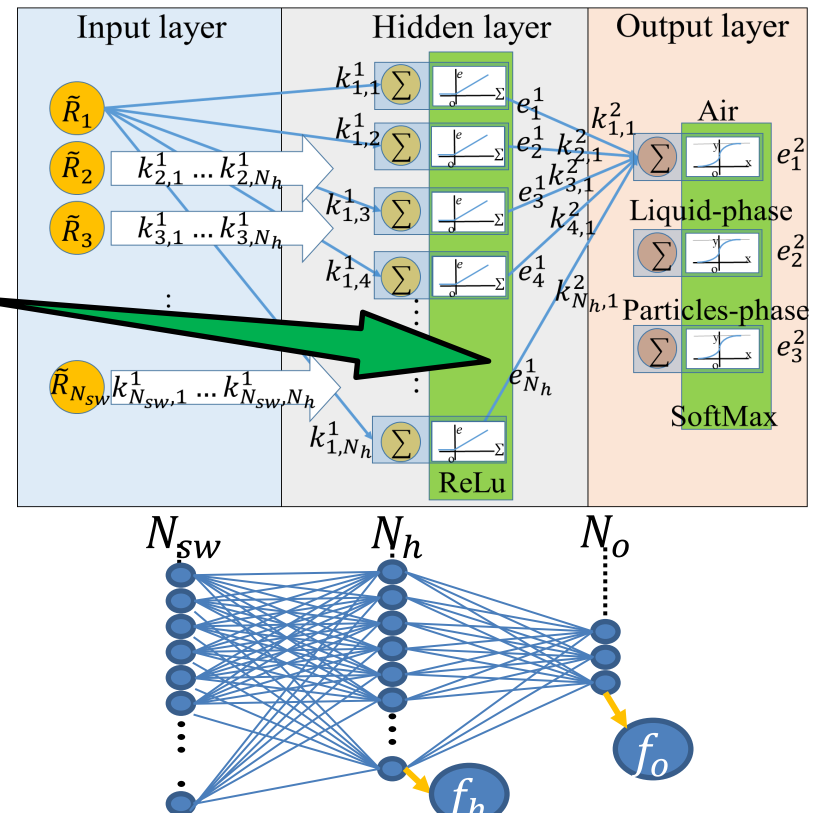

Fig. ANN architecture

Experiment component by *ls*WERT (Step 5)

Constant values	
Density of liquid	ρ_L
Density of particle	ρ_P
Beads-particle diameter	d_P

Variable	
Beads-particle number	N_P
Rotational speed	ω

lsWERT Device

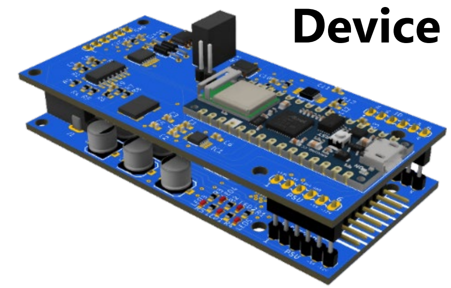

Step 5: Experimental resistance by *ls*WERT

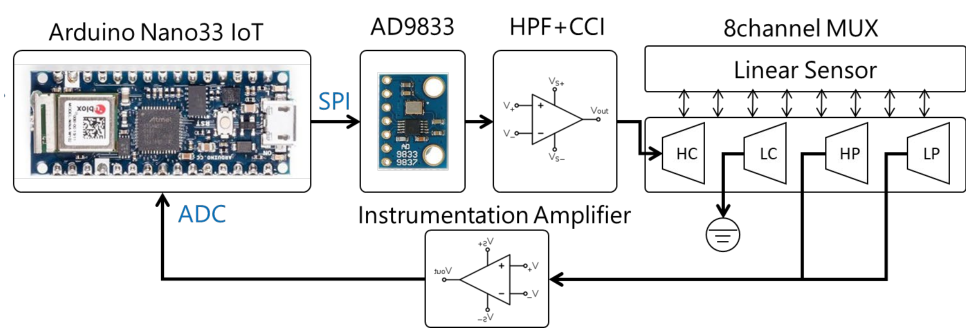

Fig. Schematic diagram of *ls*WERT device

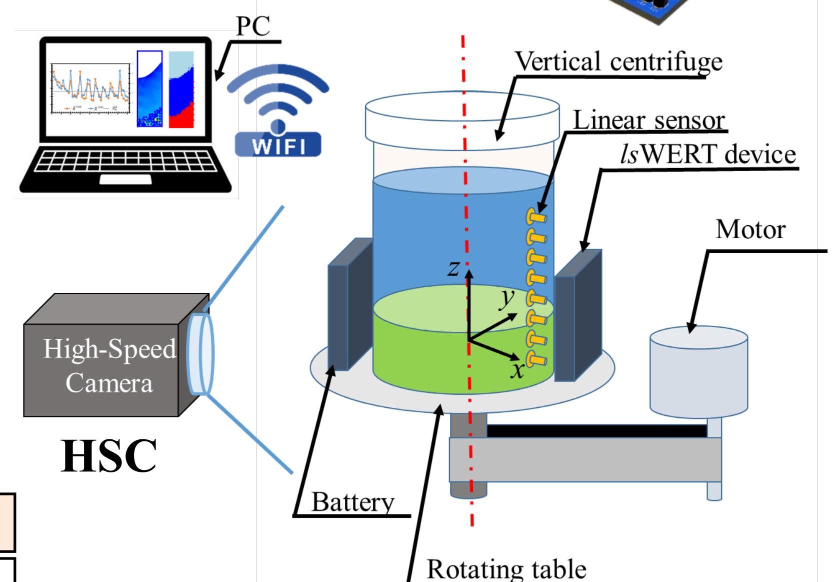

Fig. Lab-scale experimental setup

Normalized experimental resistances

Normalized experimental resistance array:

$$\widetilde{\mathbf{R}}^{exp} = \mathbf{R}^{exp} / \breve{\mathbf{R}}^{exp} \in \mathbb{R}^{N_{sw}}$$

$$\widetilde{\mathbf{R}}^{exp} = \left[R_1^{exp}, \ldots R_{n_{sw}}^{exp}, \ldots R_{N_{sw}}^{exp} \right]^T \in \mathbb{R}^{N_{sw}}$$

$\widetilde{\mathbf{R}}^{exp}$

Step 6: Phase-particles array prediction

Predicting component of phase-particles array (Step 6)

Step 5: Experimental resistance by *ls*WERT

$\widetilde{\mathbf{R}}^{exp}$

Step 4: Training component of model factors by ANN

$k_{i,j}^{n}, \beta_{j}^{n}$

Step 6: Phase-particles array prediction

$$\hat{\mathbf{x}}_1 = \left[\left(\hat{x}_{\lambda_1}, \hat{z}_{\lambda_1}\right)\right]^T$$

$$\hat{\mathbf{x}}_2 = \left[\left(\hat{x}_{\lambda_2}, \hat{z}_{\lambda_2}\right)\right]^T$$

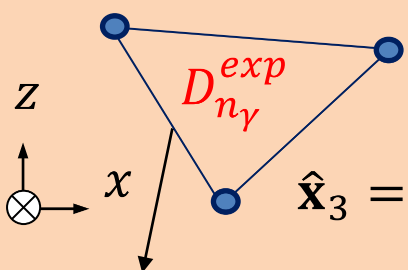

$$\hat{\mathbf{x}}_3 = \left[\left(\hat{x}_{\lambda_3}, \hat{z}_{\lambda_3}\right)\right]^T$$

$$\boldsymbol{\gamma}_n = \left[\gamma_{\lambda_1}, \gamma_{\lambda_2}, \gamma_{\lambda_3}\right] \in \mathbb{N}^3$$

$\mathbf{D}^{exp}$

Experimental phase-particles

Experimental phase-particles array:

$$\mathbf{D}^{exp} = \left[D_1^{exp}, \dots D_n^{exp}, \dots D_{N_\gamma}^{exp}\right] \in \mathbb{R}^{N_\gamma}$$

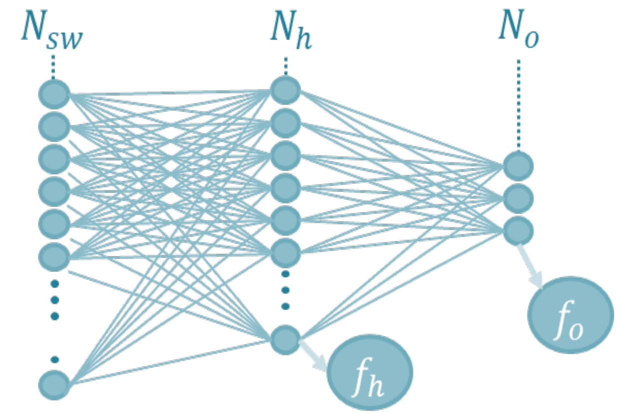

Fig. Trained ANN

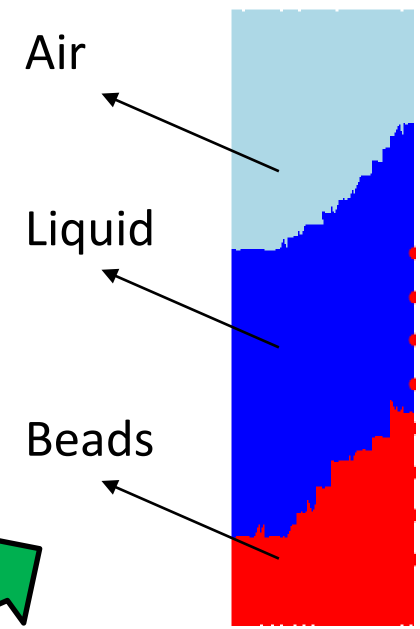

Fig. Particles deposition imaging

Experimental Results #1

Case 1: Beads-particle number $N_P\ [-] = 40$

ω [rpm]	$\mathbf{D}^{exp}$	$\mathbf{D}^{sim}$	HSC	ω [rpm]	$\mathbf{D}^{exp}$	$\mathbf{D}^{sim}$	HSC
175	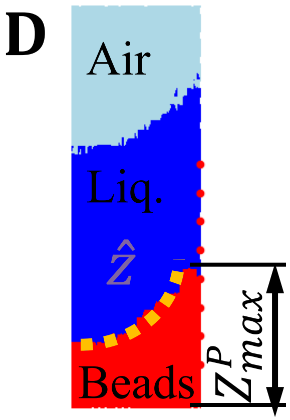	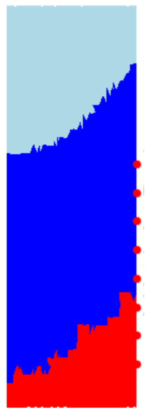	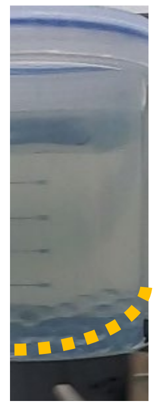	235	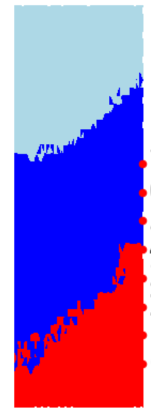	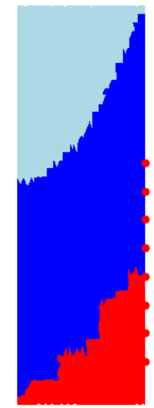	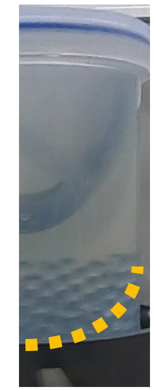
205	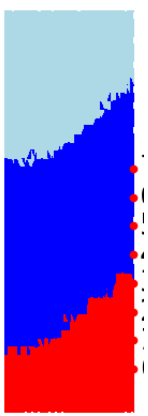	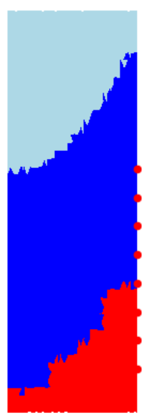	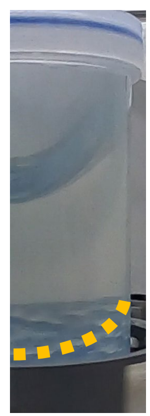	265	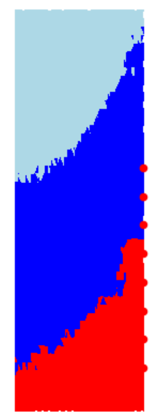	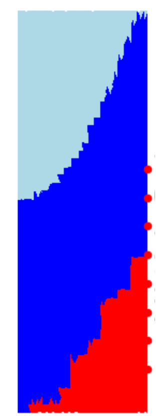	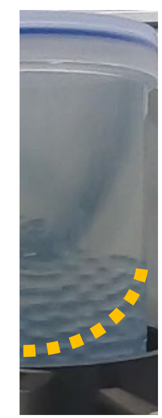

Experimental Results #2

Case 2: Beads-particle number $N_P\ [-] = 48$

ω [rpm]	$\mathbf{D}^{exp}$	$\mathbf{D}^{sim}$	HSC	ω [rpm]	$\mathbf{D}^{exp}$	$\mathbf{D}^{sim}$	HSC
175	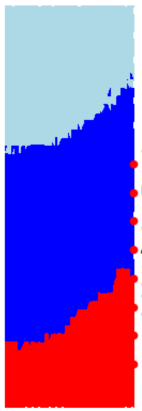	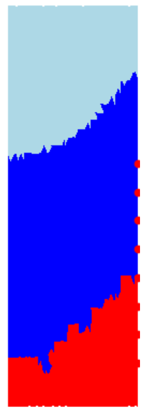	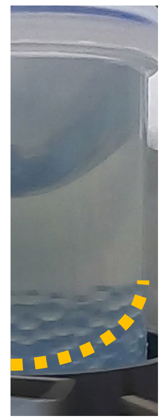	235	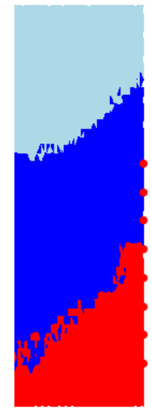	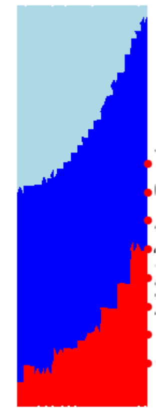	
205	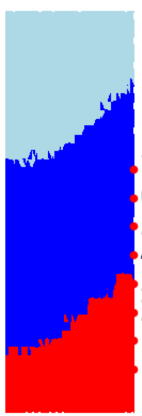	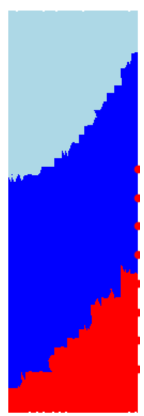		265	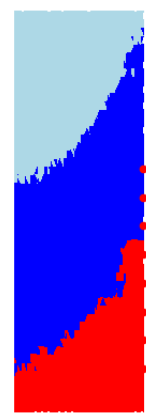	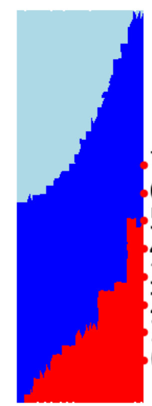	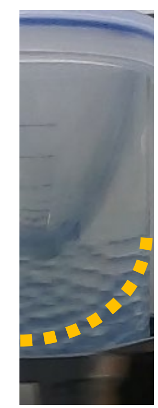

Experimental Results #3

Case 3: Beads-particle number N_P [−] = 56

ω [rpm]	$\mathbf{D}^{exp}$	$\mathbf{D}^{sim}$	HSC
175	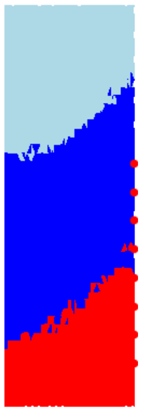	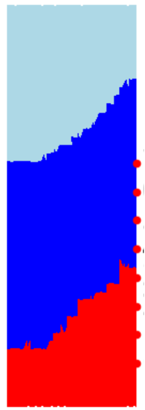	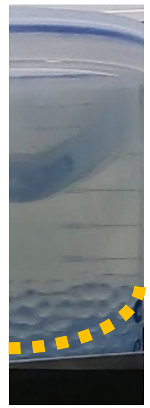
205	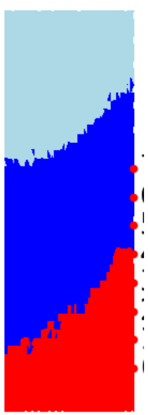	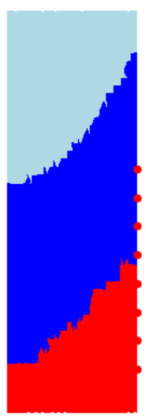	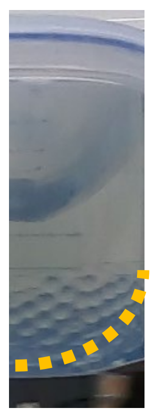

ω [rpm]	$\mathbf{D}^{exp}$	$\mathbf{D}^{sim}$	HSC
235	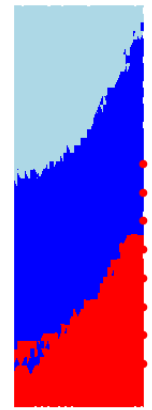	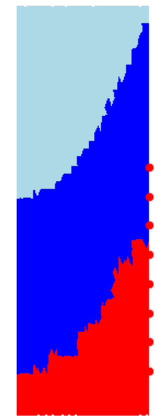	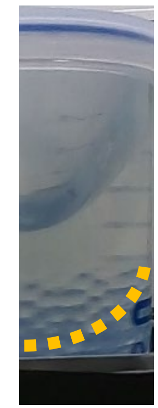
265	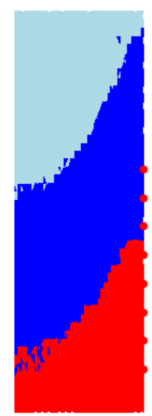	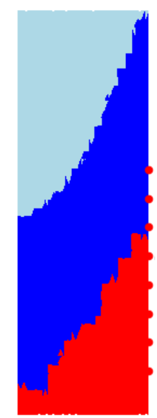	

Discussion: Comparison with HSC

$$RMSE = \sqrt{\frac{1}{N_{ch}} \sum_{n_{ch}=1}^{N_{ch}} \left(\hat{z}_{n_{ch}}{}^{exp} - \hat{z}_{n_{ch}}{}^{true} \right)^2}$$

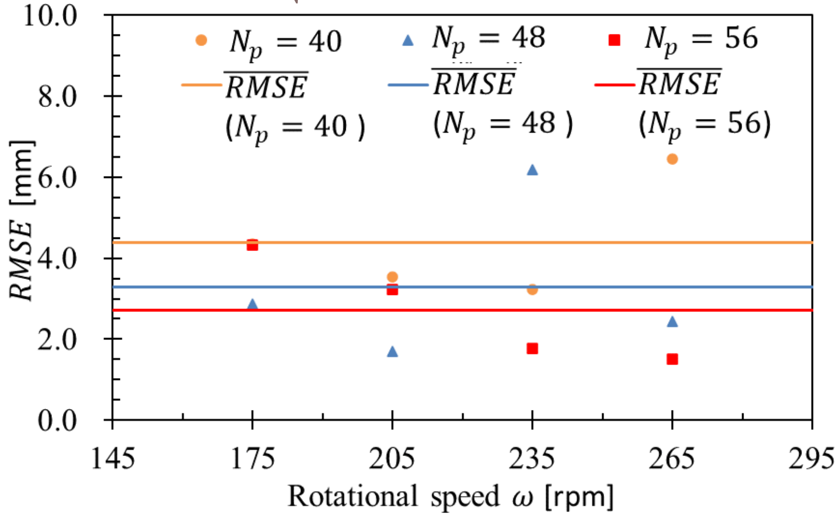

N_P [−] = 40

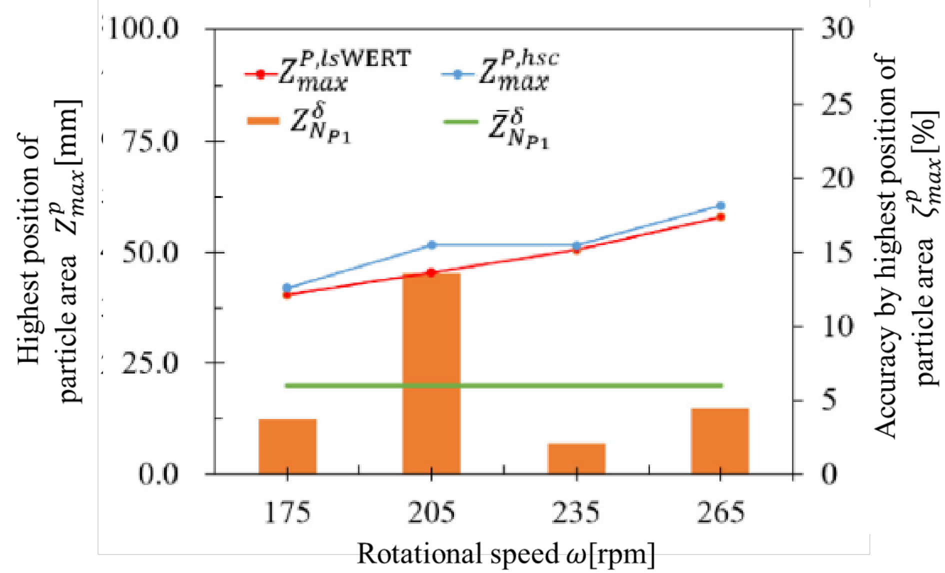

N_P [−] = 48

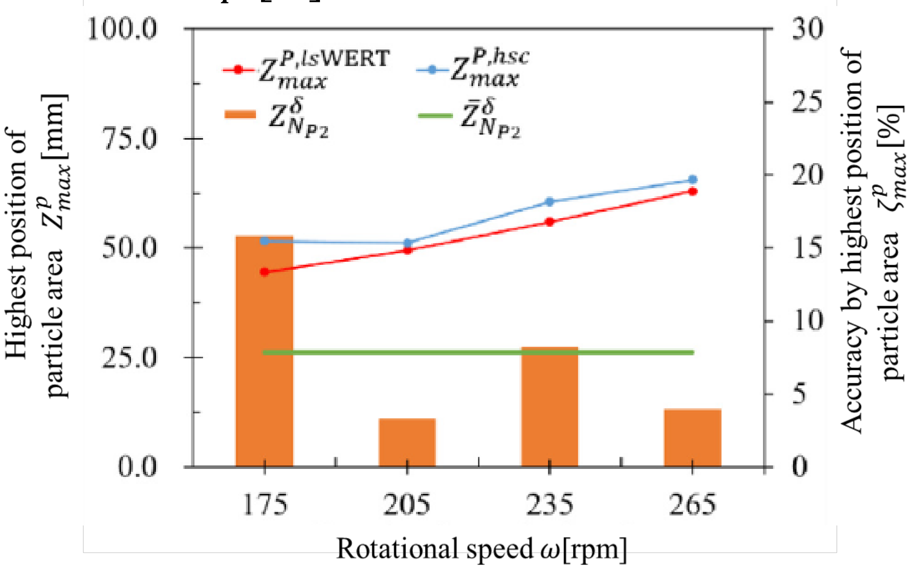

N_P [−] = 56

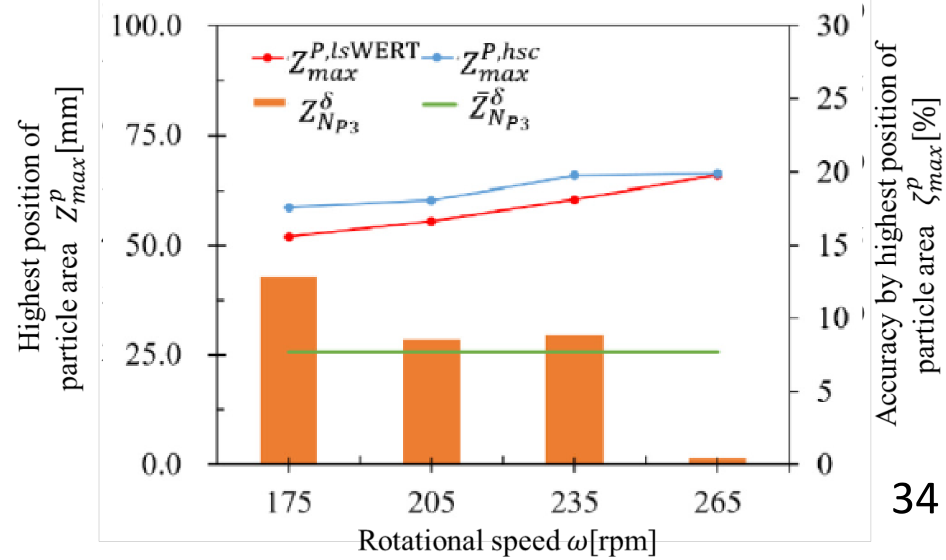

OUTLINE

TAKEI Laboratory
武居　研究室
Laboratory on Multiphase Flow and Visualization

UNIVERSITAS GADJAH MADA

✓Overview of Electrical Impedance Tomography[1] (5 min)

✓ ***In situ* measurement on industrial decanter by Wireless Electrical Resistance Tomography (WERT)[2-6] (40 min)**

✓ **Development of Lymphedema Monitor (10 min)**

✓ **Concluding Remarks and Questions (5 min)**

[2]Y. Atagi and M.Takei, real-time imaging of particles distribution in centrifugal particles-liquid two phase fields by wireless electrical resistance tomography (WERT) system, *IEEE Access*, Vol. 7. pp.12706 - 12713 (2019)

[3]K. Kimura, Y.A.K. Prayitno, and M. Takei, In situ particles deposition imaging in centrifugal fields by implemented SPH-DEM-ANN into linear sensor-type wireless electrical resistance tomography (lsWERT), *Powder Tech.*, Vol. 398, 117140 (2022)

[4]Z. Tong and M. Takei, real-time measurement of particle volume fraction in centrifugal fields by wireless electrical resistance detector (WERD), *Flow Meas. and Inst.*, 65, 90-97 (2018)

[5]Y. A. K. Prayitno and M. Takei, in-situ measurement of sludge thickness in high-centrifugal force by optimized particle resistance normalization for wireless electrical resistance detector (WERD), *Measurement Sci. & Tech.*, 32(3), 034001 (2020)

[6]Y.A.K. Prayitno and M. Takei, *In situ* measurement of hindered settling function in decanter centrifuge by periodic segmentation technique in wireless electrical resistance detector (*ps*WERD), *Advanced Powder Tech.*, 33(1), 103370 (2021)

Overview of WERD: Research Background

TAKEI Laboratory
武居 研究室
Laboratory on Multiphase Flow and Visualization

Current issues | Technical problems | Research target

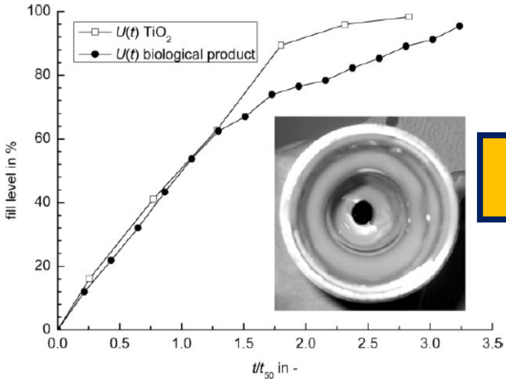

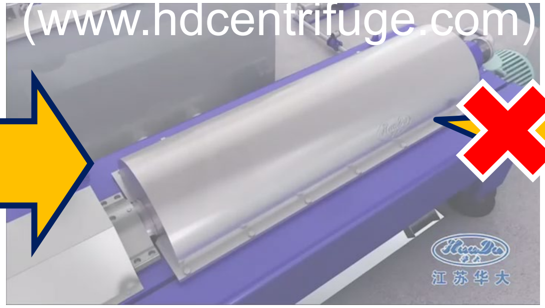

Decanter

In situ meas. **device**

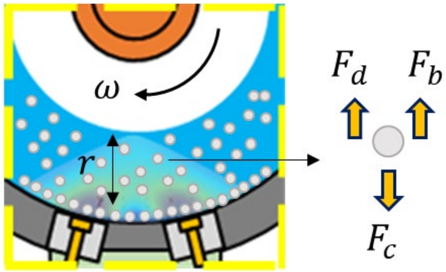

***In situ* particles settling** in decanter by **WERD**

Indirect separation evaluation ≠ **real-time**
Stahl et al., *Chem. Eng. Tech.* (2008)

Research History

<2019 → 2020

1st version of WERD[4]

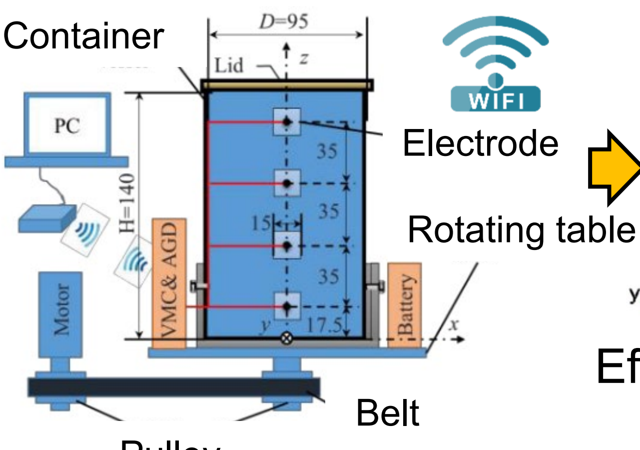

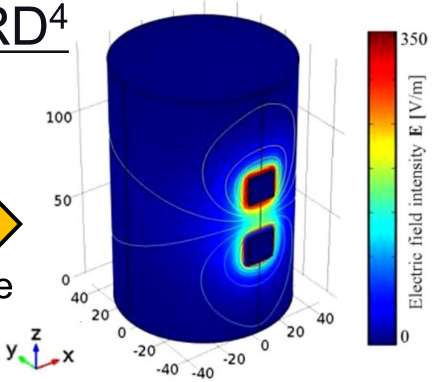

Effective sensing area

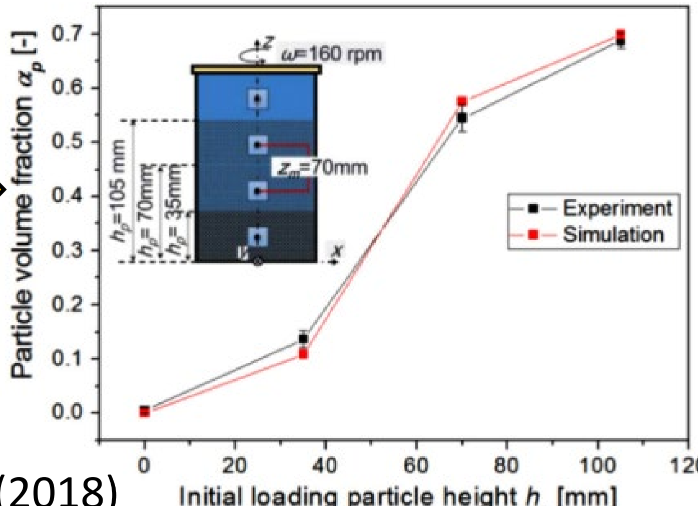

[4]T. Zhao and M. Takei, *Flow Meas. and Inst.* (2018)

Overview of WERD: Research History

<2020 → 2021

2nd version of WERD[5]

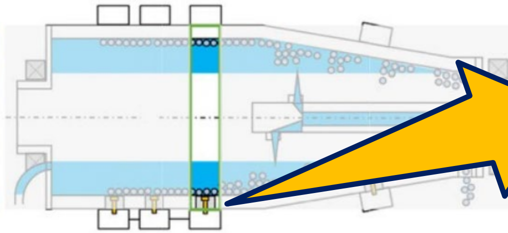

WERD

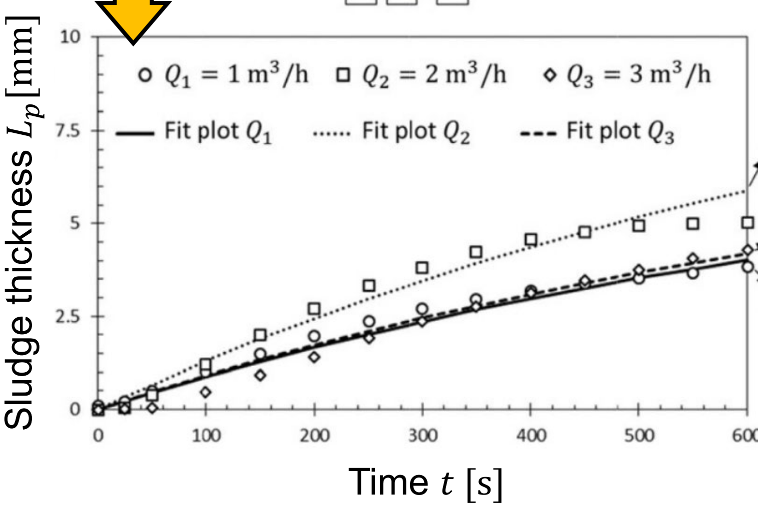

Sludge thickness

Optimized Particle Resistance Normalization[3]

$$R_{N(L_p)} = \frac{R_{x(L_p)} - R_{ref}}{R_{x(L_p\,\mathrm{Max})} - R_{ref}}$$

$$f(L_p) = \xi \cdot \ln\left(1 - \frac{R_{N(L_p)}}{k}\right)$$

Minimize

$$f(R_{N(L_p)}) = f(\mathbf{R})$$

Partitioned

$$\overline{\mathbf{R}} = (\bar{y}, \bar{x}) = (\overline{R_N}, \overline{L_p})$$

Boundary

$$l_{NB} \le R_{N(L_p)} \le u_{NB}$$

Fitted

$$F(x) = f(\xi y(x), kx) = f(R_{N(L_p)}, L_p)$$

$R_{N(L_p)}$ [−]: Normalized Resistance

$R_{x(L_p)}$ [Ω]: Measured Resistance

R_{ref} [Ω]: Reference Resistance

$R_{x(L_p\,\mathrm{Max})}$ [Ω]: Resistance of max. thickness

l_{NB} [−]: Lower normalized boundary

u_{NB} [−]: Upper normalized boundary

ξ, k [−]: OPRN Coeff.

[5]Y.A.K Prayitno and M. Takei, *Meas. Sci. and Tech.* (2020)

In situ hindered settling function by WERD[6]

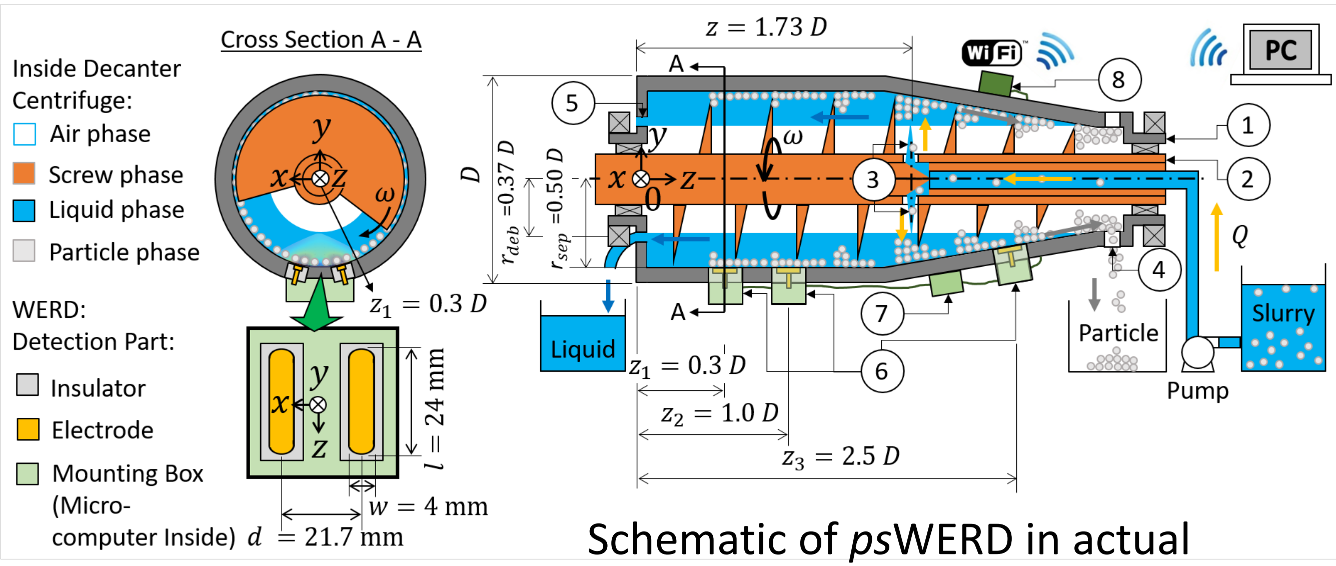

Schematic of *ps*WERD in actual decanter centrifuge

Actual decanter-WERD:

1) Bowl
2) Screw conveyor
3) Feed inlet
4) Particle outlet
5) Liquid outlet
6) Detection part
7) Power supply part
8) Communication part

Period segmentation WERD (*ps*WERD)

- Step 1 : Segmentation of $R(t)$
- Step 2 : Elimination of SC's adverse effect
- Step 3 : Calculation of ϕ
- Step 4 : Calculation of $H(\phi)$

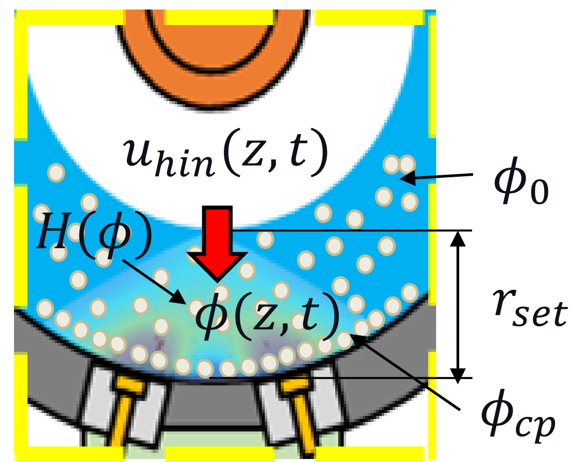

[6]Y.A.K Prayitno and M. Takei, *Adv. Powd. Tech.* (2022)

Period segmentation WERD (*ps*WERD) #1

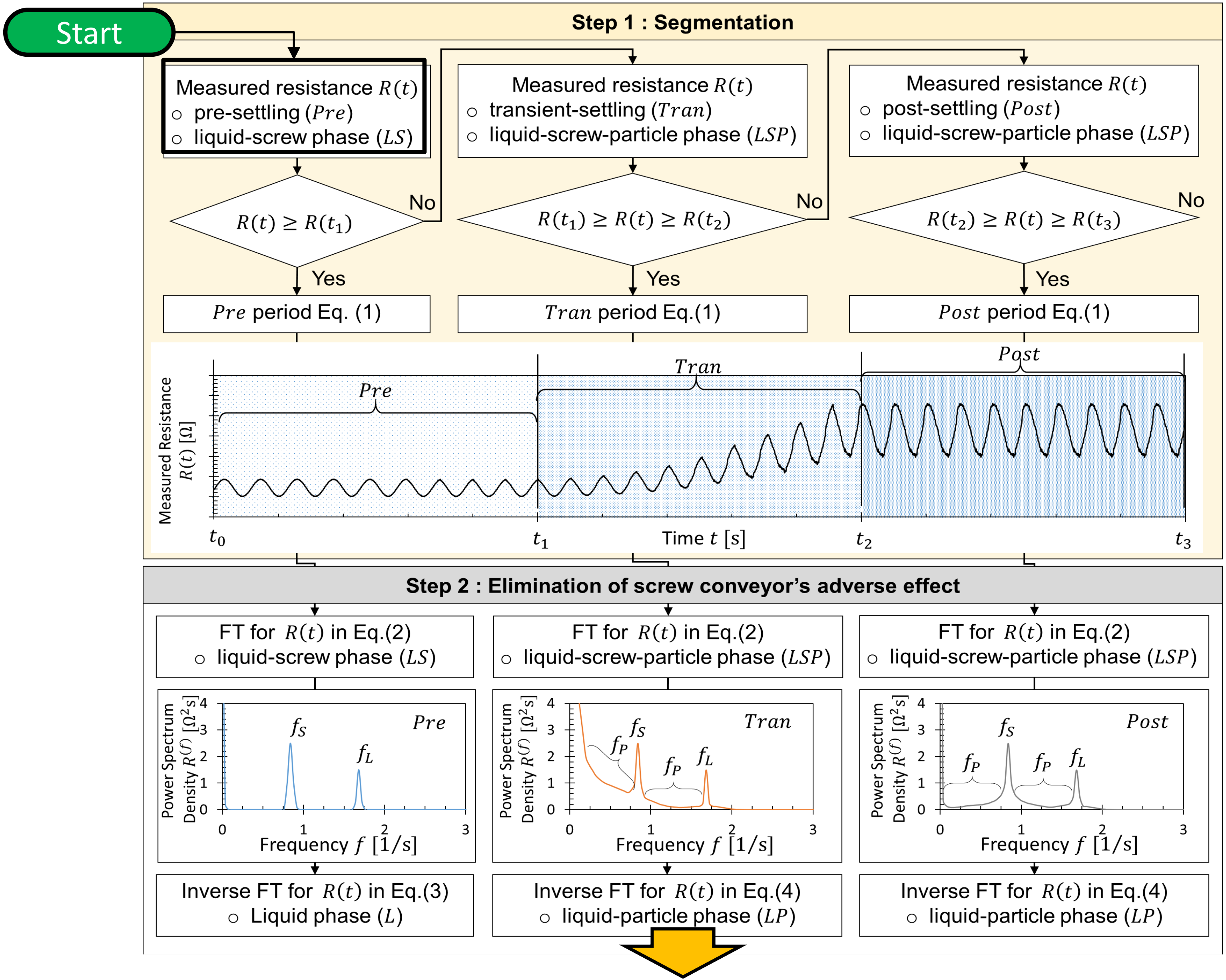

Period segmentation WERD (*ps*WERD) #2

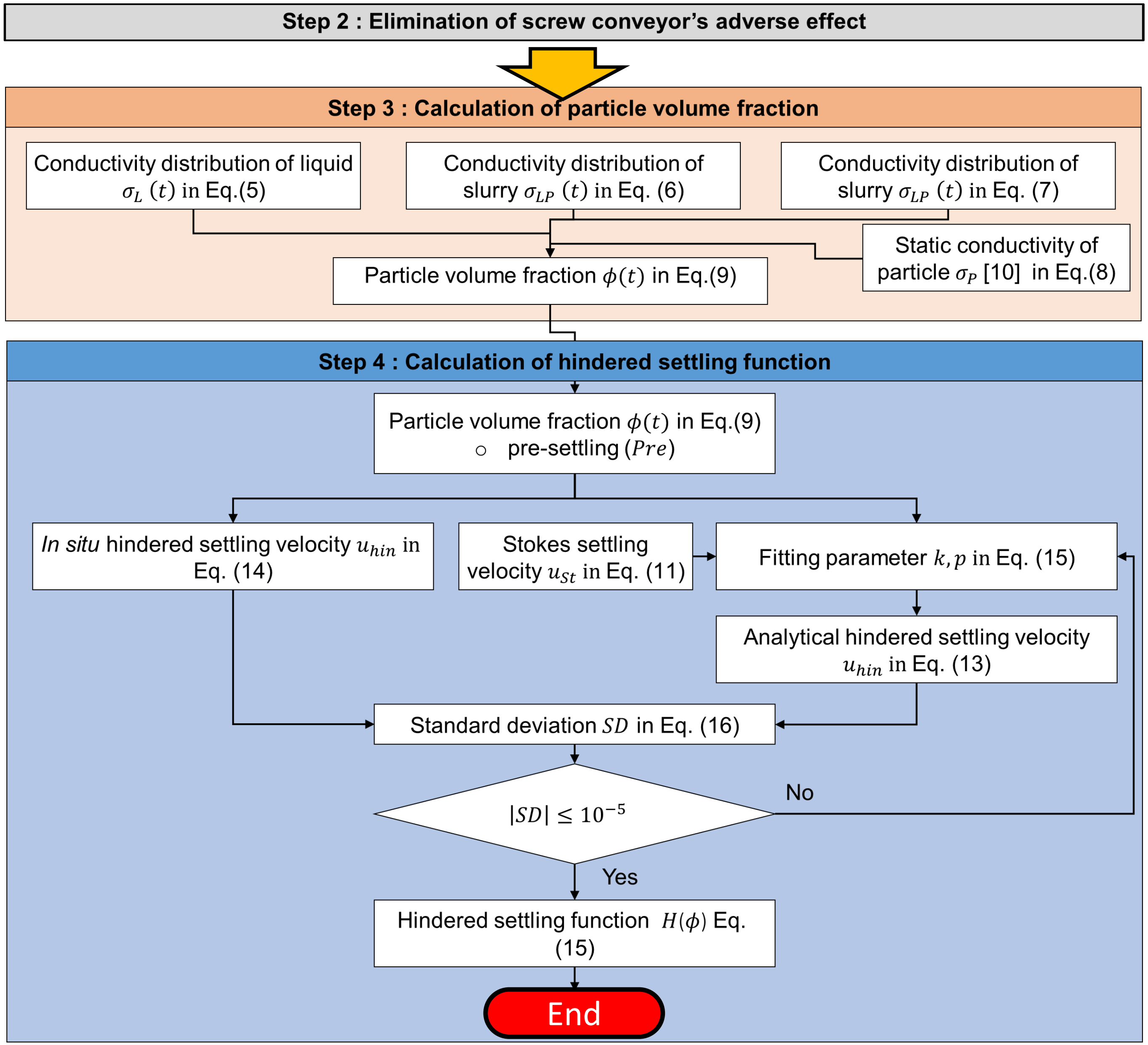

Step 1: Segmentation of $R(t)$

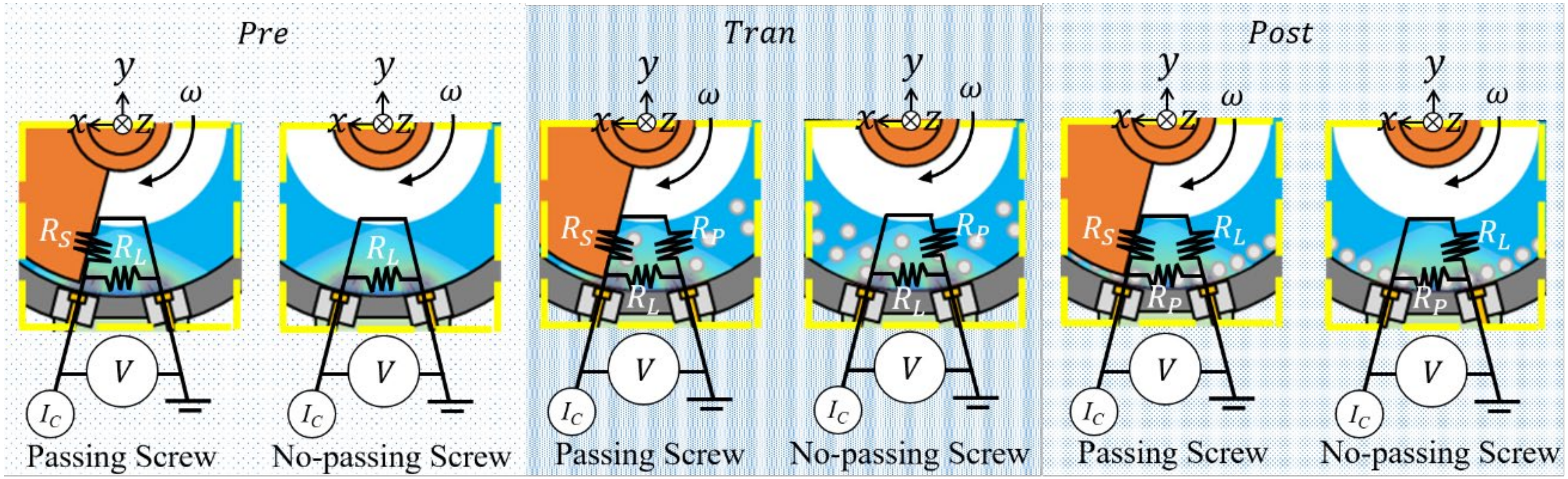

Simplified EEC model in three settling conditions

pre = no supplied particle $tran$ = supplied particle $post$ = saturated

Measured by WERD

$$R(z,t) = \begin{cases} R(z,t) \text{ in } pre \ t_0 \le t \le t_1 \\ R(z,t) \text{ in } tran \ t_1 \le t \le t_2 \\ R(z,t) \text{ in } post \ t_2 \le t \le t_3 \end{cases} \quad (1)$$

at measurement points $z_1 \le z \le z_3$

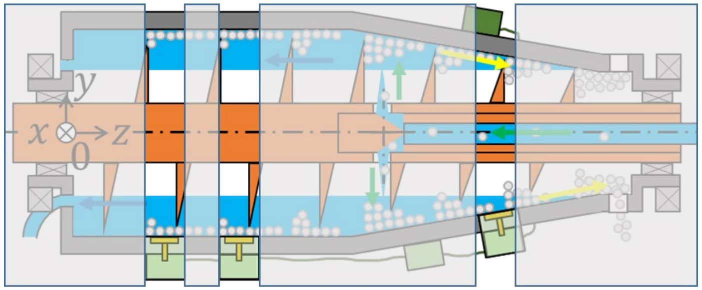

$R(z,t)[\Omega]$: Measured resistance in different point and time

$z[\text{mm}]$: Measurement point $t[s]$: Measurement time

Step 2: Elimination of SC's adverse effect

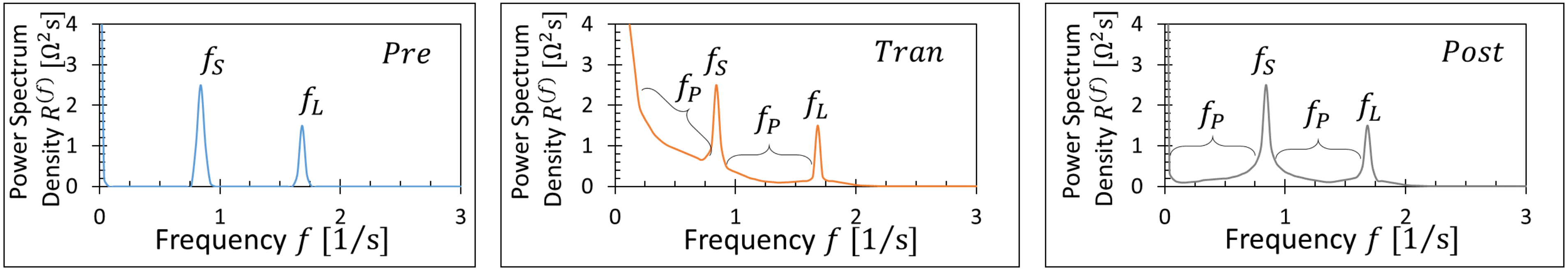

FFT in three settling conditions

$$\bar{R}(\mathbb{Z},\omega) = \int_{z_n}^{z_n}\int_{t_n}^{t_{n+1}} R(z,t)e^{-i(\mathbb{Z}z+\omega t)}dzdt \quad (2)$$

Differential speeds ω affects the fluctuating $R(t)$ under settling periods

$$R_L(z,t) = \frac{1}{2\pi}\int_{\mathbb{Z}}^{\mathbb{Z}}\int_{f_L}^{f_S} \bar{R}(\omega)e^{i(\mathbb{Z}z+\omega t)}d\mathbb{Z}d\omega \text{ in } t_0 \le t \le t_1 \quad (3)$$

$$R_{LP}(z,t) = \frac{1}{2\pi}\int_{\mathbb{Z}}^{\mathbb{Z}}\int_{f_{LP}}^{f_S} \bar{R}(\omega)e^{i(\mathbb{Z}z+\omega t)}d\mathbb{Z}d\omega \text{ in } t_1 \le t \le t_3 \quad (4)$$

$\bar{R}[\Omega^2 s]$: Measured resistance in frequency domain

R_L $[\Omega]$: Liquid resistance R_{LP} $[\Omega]$: Slurry resistance

f_L $[1/s]$: liquid frequency f_S $[1/s]$: screw frequency f_P $[1/s]$: particle frequency

Step 3: Calculation of particle volume fraction ϕ

$$\sigma_L(z,t) = \frac{1}{R_L\ (z,t)} \frac{d}{A_{Elc}} \quad (5)$$

$$\sigma_P = \frac{1}{R_P} \frac{l}{A_{Elc}}\ ; R_P \text{ at } \phi_{cp} \quad (6)$$

$$\bar{\sigma}_L(z,t) = \frac{1}{N} \sum_{t_0}^{t_1} \sigma_L(z,t) \text{ in } t_0 \leq\ t \leq t_1 \text{ and } z_1 \leq z \leq z_3 \quad (7)$$

$$\sigma_{LP}(z,t) = \frac{1}{R_{LP}\ (z,t)} \frac{d}{A_{Elc}} \text{ in } t_1 \leq\ t \leq t_2 \text{ and } z_1 \leq z \leq z_3 \quad (8)$$

$$\sigma_{LP}(z,t) = \frac{1}{R_{LP}\ (z,t)} \frac{d}{A_{Elc}} \text{ in } t_2 \leq\ t \leq t_3 \text{ and } z_1 \leq z \leq z_3 \quad (9)$$

Effective medium theory (EMT): Relationship of conductivity σ and volume fraction ϕ by complex multiphase mixture

Maxwell, *Cambridge Univ. Press* (2010)

$$\phi(z,t) = \frac{\bar{\sigma}_L\sigma_P - \sigma_P\sigma_{LP}(z,t)}{\bar{\sigma}_L\sigma_{LP}(z,t) - \sigma_P\sigma_{LP}(z,t)} \quad (10)$$

$\sigma_L[\mathrm{Sm}^{-1}]$: Liquid conductivity

$\sigma_{LP}[\mathrm{Sm}^{-1}]$: Slurry conductivity

$\sigma_P[\mathrm{Sm}^{-1}]$: Closed-pack particle conductivity

$\bar{\sigma}_L[\mathrm{Sm}^{-1}]$: Liquid relative conductivity

$d[\mathrm{mm}]$: Electrode distance

$A_{Elc}[\mathrm{mm}^2]$: Electrode area

$\phi_{cp}[-]$: Closed-pack particle volume fraction

$\phi[-]$: Particle volume fraction

Step 4: Calculation of $H(\phi)$

$H(\phi)$: Decanter's particle settling $\neq$ Stokes settling velocity u_{St}

$$u_{St} = \frac{(\rho_p - \rho_l)a^2 g}{18\mu_l} \quad (11)$$

$$G = \frac{\omega^2(r_{sep} - r_{deb})}{g} \quad (12)$$

$$u_{hin} = \frac{H(\phi)(\rho_p - \rho_l)a^2\omega^2(r_{sep} - r_{deb})}{18\mu_l} \quad (13)$$

$$u_{hin}^{ins}(z,t) = \frac{r_{set}(\phi(z,t))}{\Delta t} = \frac{r_{set}(\phi_{cp}(z,t) - \phi_0(z,t))}{t_2 - t_1} \quad (14)$$

$$H(\phi(z,t)) = \frac{u_{hin}(z,t)}{u_{St}} = \left(1 - k\left(\frac{\phi(z,t)}{\phi_{cp}}\right)\right)^p \quad (15)$$

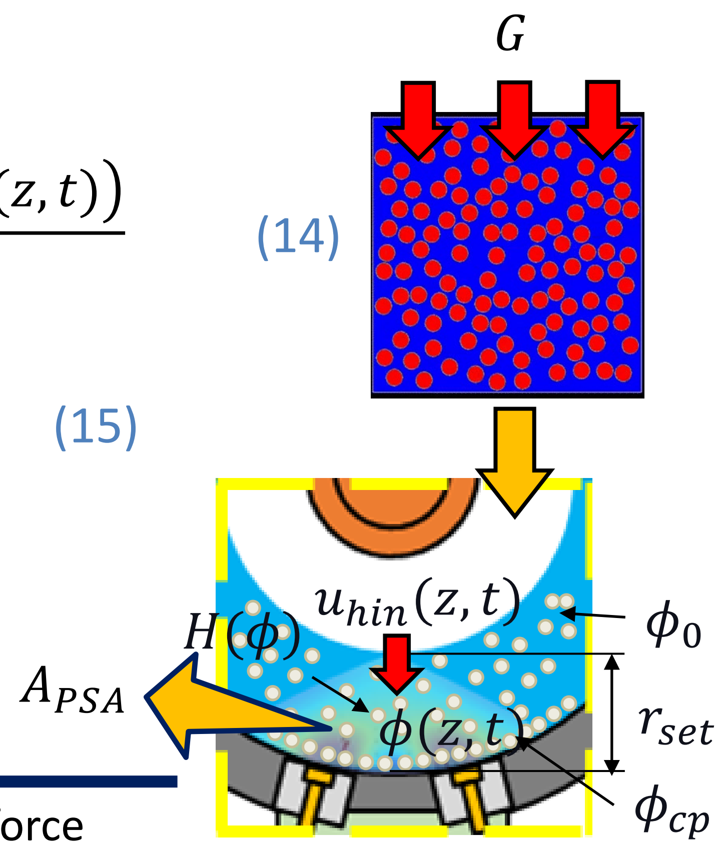

Assumption:

- Settling radius r_{set} = clearance between screw conveyor SC and bowl $\approx 1 - 1.5$ mm in A_{PSA}
- Settling time in $r_{set}(\phi(z,t))$ → determine u_{hin}

$H(\phi)[-]$: Hindered settling function

$u_{St}\ [\mathrm{mms^{-1}}]$: Stokes settling velocity

$u_{hin}[\mathrm{mms^{-1}}]$: Hindered settling velocity

$G[g]$: centrifugal force

$k, p[-]$: coefficient of $H(\phi(z,t))$

$u_{hin}^{ins}[\mathrm{mms^{-1}}]$: *In situ* hindered settling velocity

Industrial-Scale Experiments of $H(\phi)$ by WERD

Setup and Conditions

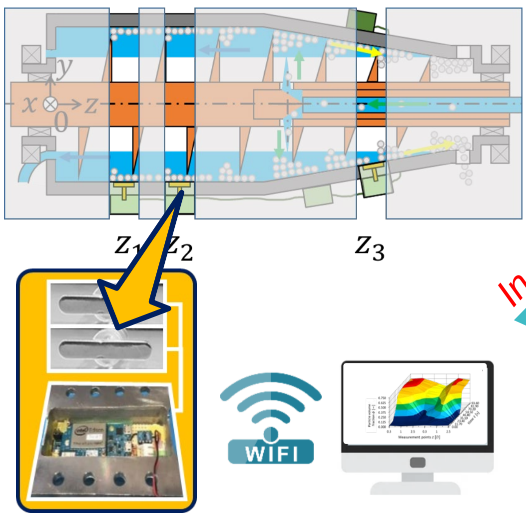

Fig. Decanter-WERD setup

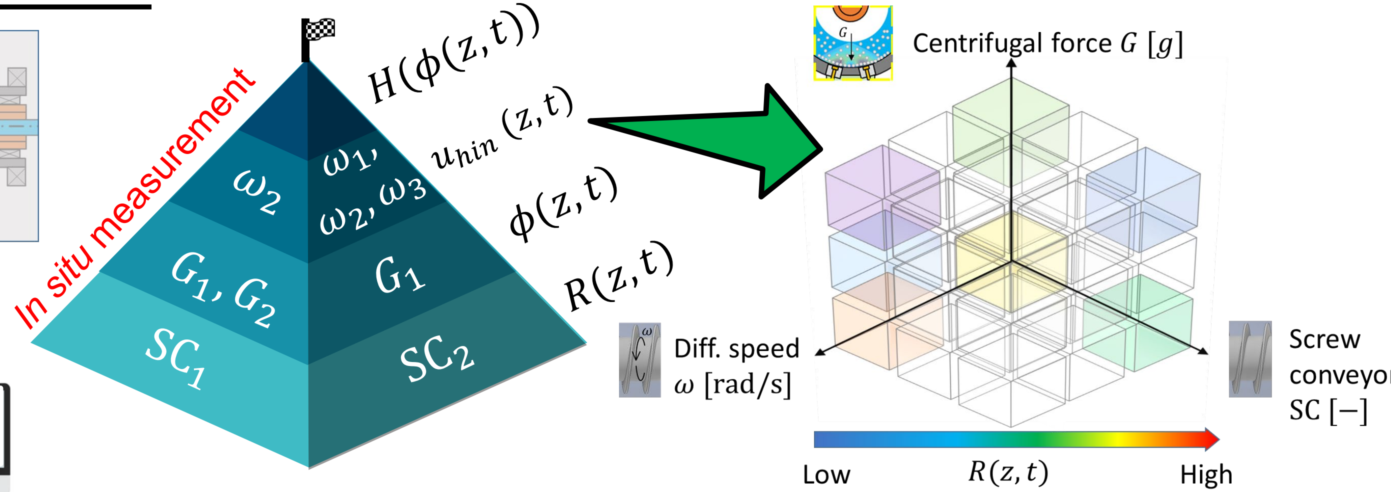

Fig. Experiments condition

Centrifugal force G

Parameter	Value
G_1 $[g]$	1,075.3
G_2 $[g]$	2,129.9

Configuration of SC

Parameter	a/b
SC1 $[-]$	0.4375
SC2 $[-]$	0.2222

Diff. speed of SC

Parameter	Value
ω_1 [rad/s]	0.524
ω_2 [rad/s]	1.047
ω_3 [rad/s]	3.142

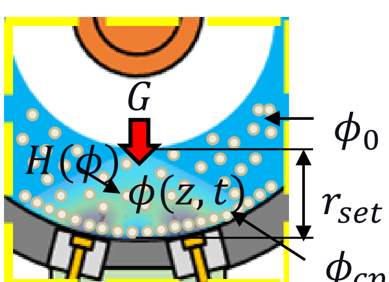

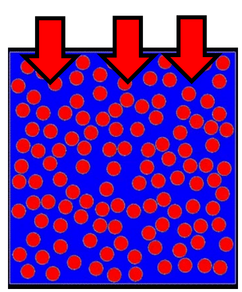

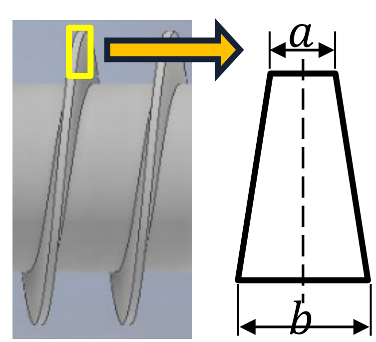

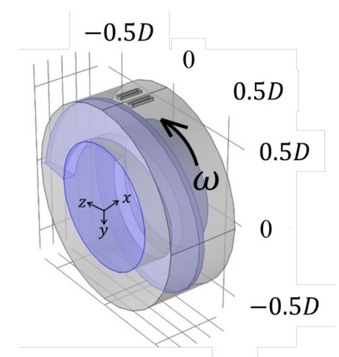

Results: Effect of SC to WERD

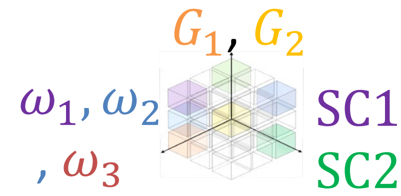

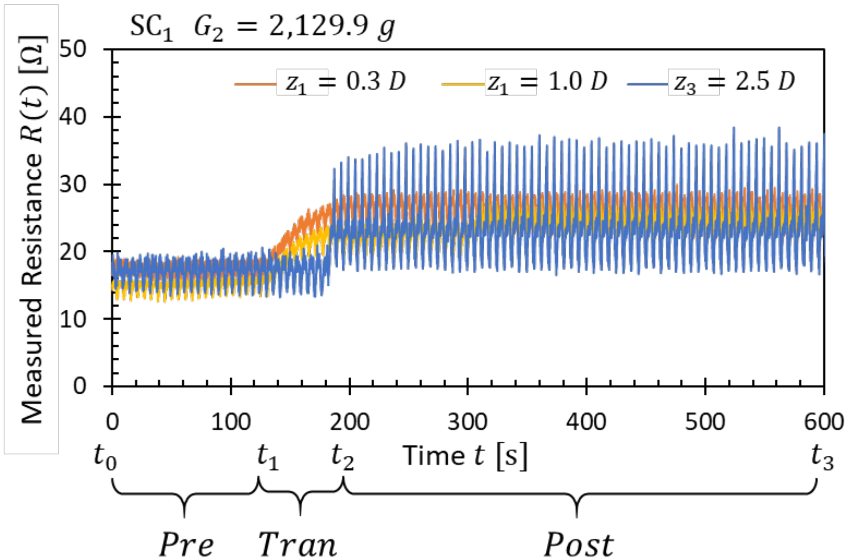

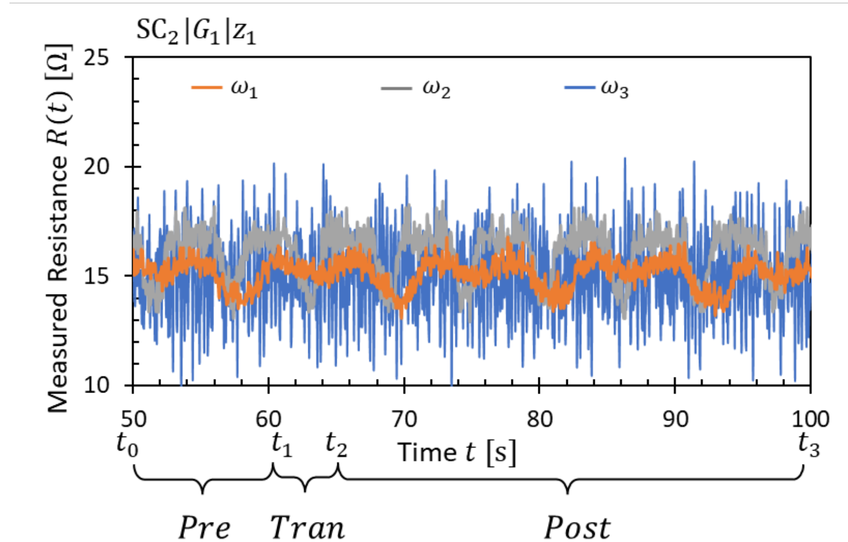

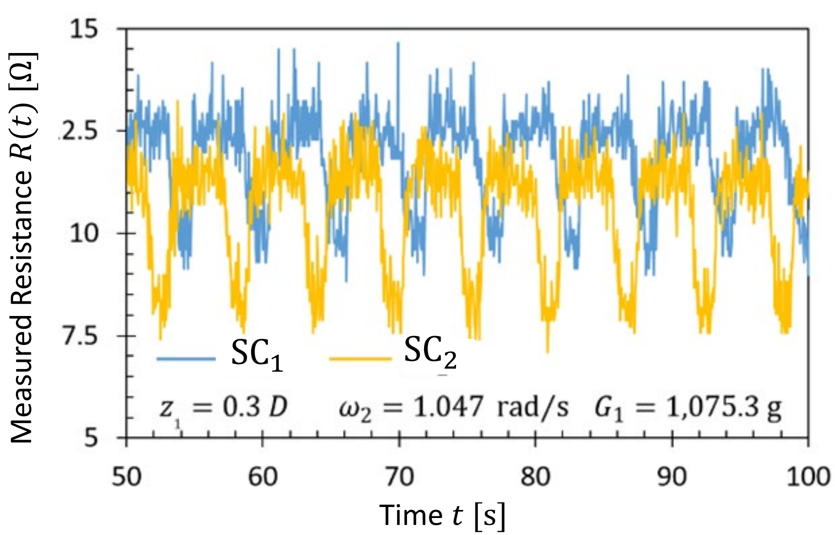

- Different SC → fluctuating $R(t) \approx$ sinusoidal wave
- The peaks and lows → passing screw and no-passing screw → different ω

Results: Elimination of SC's adverse effect

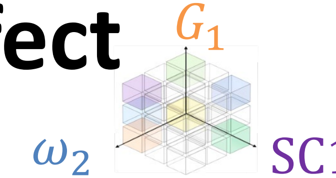

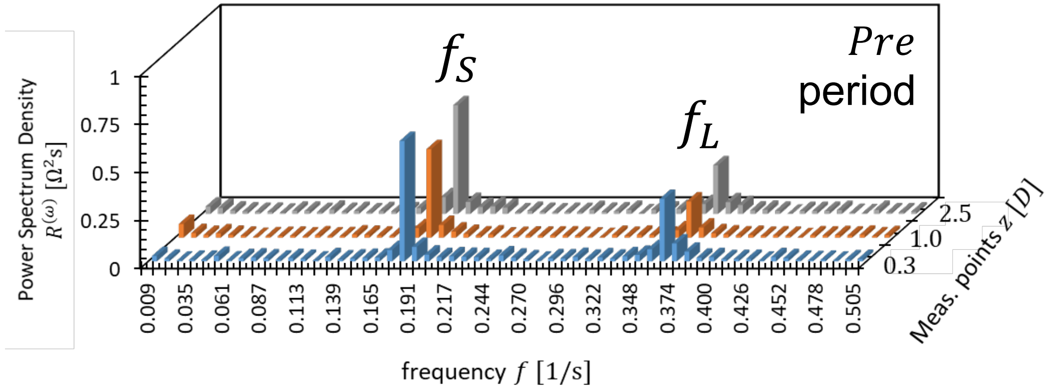

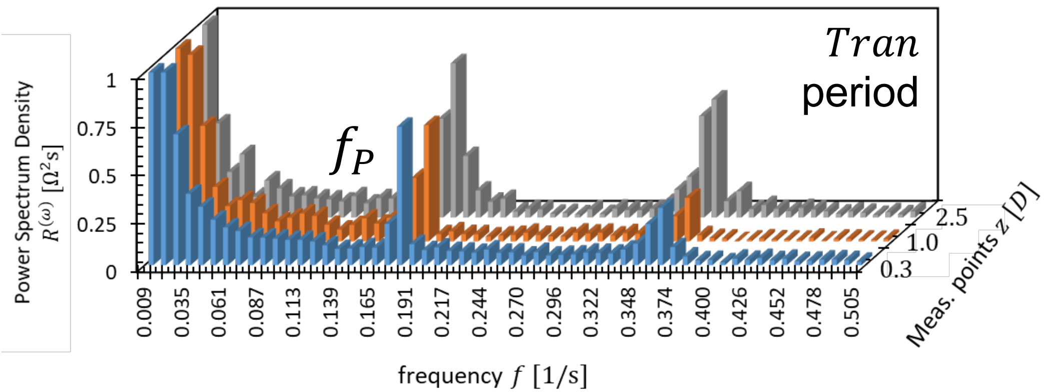

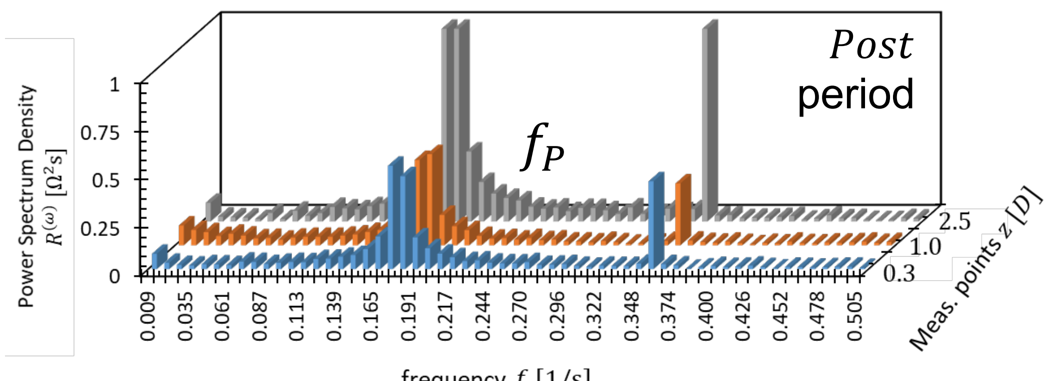

SC1

$G_1 = 1{,}075.3\ g$

$\omega_2 = 1.047\ \text{rad/s}$

- $R(t)$ in DC signal, fluctuation as the effect of ω
- In Pre period :
  - $f_S = 0.183$ [1/s]
  - $f_L = 0.365$ [1/s]
- In $Tran$ and $Post$ period :
  - $f_P = 0.009 - 0.165$ [1/s] and $0.217 - 0.348$ [1/s]
- Similar range of calculated frequency f under ω_2 as,
  - Passing screw $f = 0.167$ [1/s]
  - No−passing screw $f = 0.334$ [1/s]

Results: Transient behavior of *in situ* ϕ

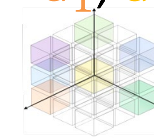

$SC1 - \omega_2 = 1.047$ rad/s $G_1 = 1{,}075.3\ g$

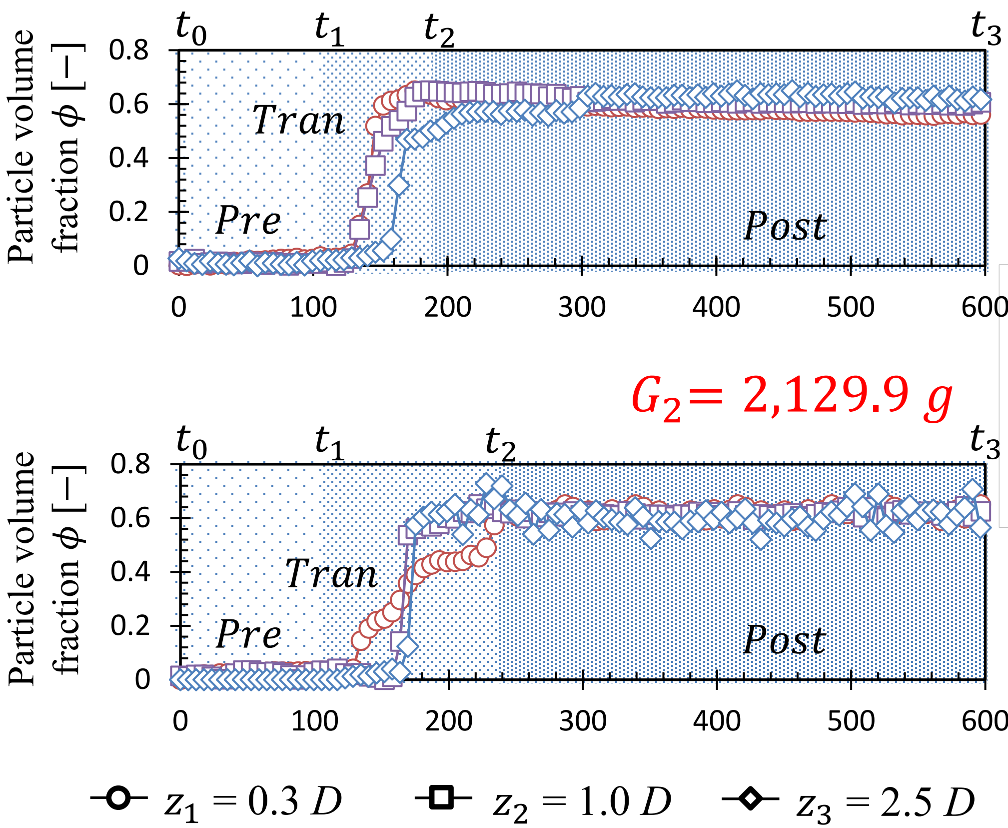

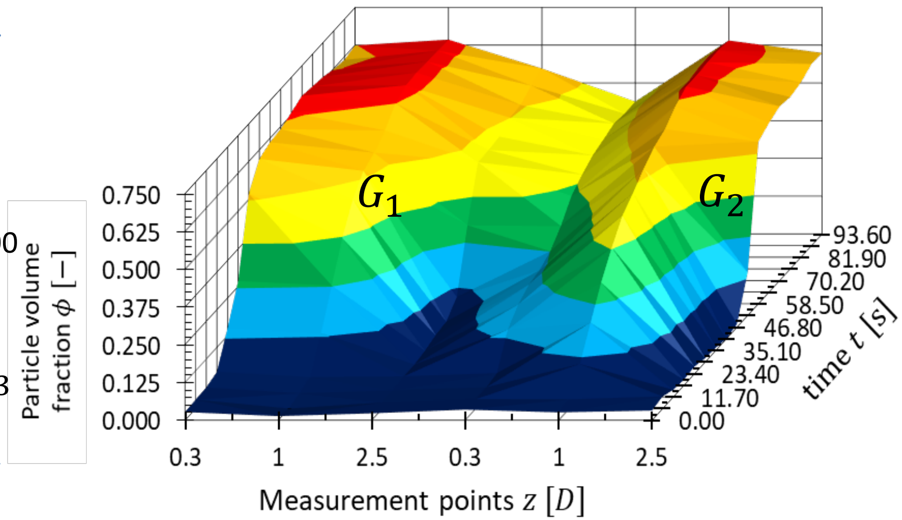

Transient behaviour of particle volume fraction ϕ for Screw conveyor 1 SC1.

ϕ [−]
- 0.000-0.125
- 0.125-0.250
- 0.250-0.375
- 0.375-0.500
- 0.500-0.625
- 0.625-0.750

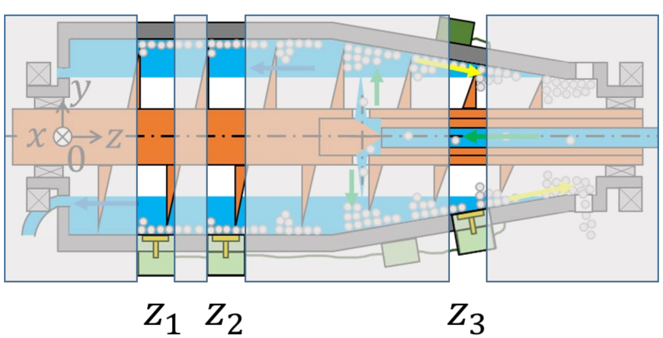

- Lower $G \rightarrow G_1 = 1{,}075.3\ g$: ϕ distributed through z_1

TAKEI Laboratory
武居 研究室
Laboratory on Multiphase Flow and Visualization

Results: Calculation of *in situ* $H(\phi)$

- Determine coefficient of k, p

$$u_{hin}^{ins} = u_{hin}(z,t) = u_{St}\left(1 - k\left(\frac{\phi(z,t)}{\phi_{cp}}\right)\right)^{p} \Rightarrow u_{hin}^{fit} \Rightarrow RMSE = \sqrt{\frac{\sum_{i=1}^{N}\left[u_{hin}^{fit} - u_{hin}^{ins}\right]^2}{N}}$$

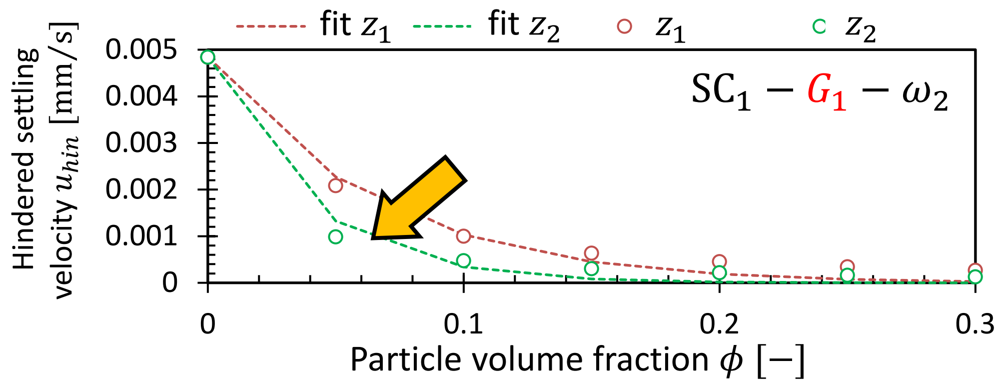

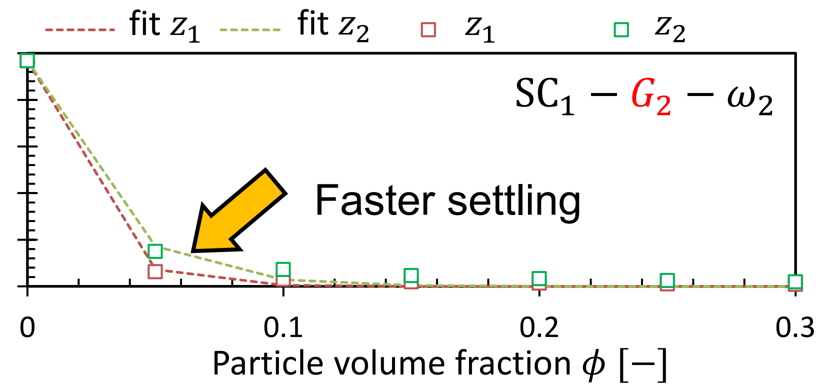

Table fitting parameter values

Experimental condition	k	p	$RMSE$
$SC_1 - G_1 - \omega_2$			
Measurement point 1 z_1 $[D]$	0.55	17.5	0.00014
Measurement point 2 z_2 $[D]$	0.55	30	0.00012
$SC_1 - G_2 - \omega_2$			
Measurement point 1 z_1 $[D]$	0.55	60	0.00005
Measurement point 2 z_2 $[D]$	0.55	40	0.00009

Discussions: Comparison to previous works

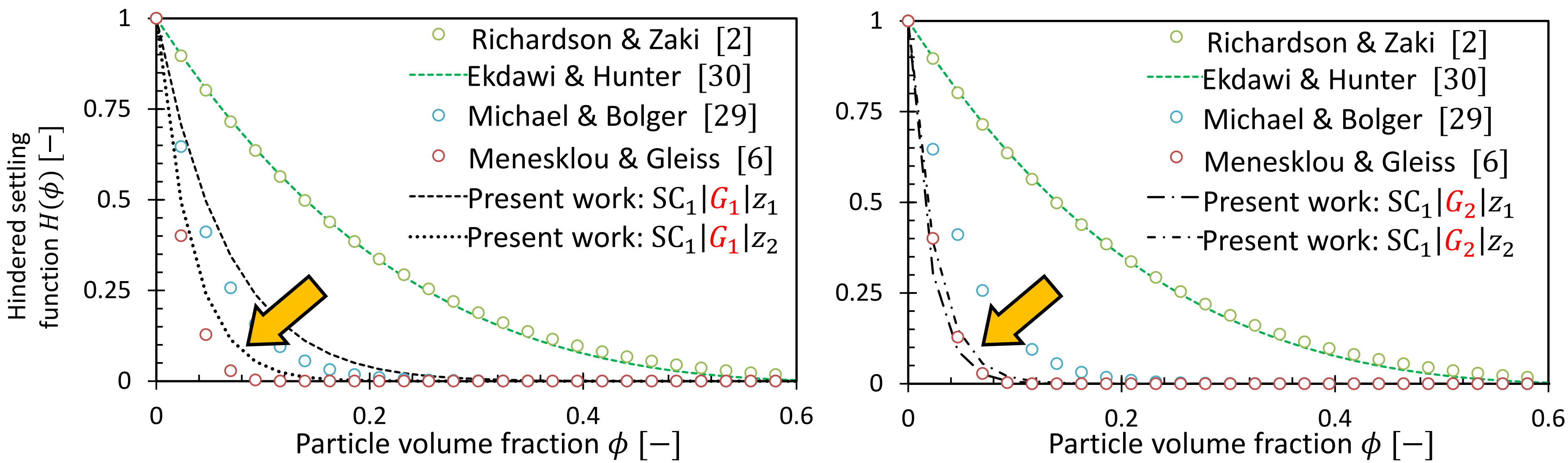

- $H(\phi)$ of Richardson & Zaki = Ekdawi & Hunter = gravitational settling
- $H(\phi)$ of Michael and Bolger = particle settling in decanter centrifuge
- $G = 1{,}000 - 2{,}000\ g$ ➡ $H(\phi)$ from Michael and Bolger, $H(\phi)$ from Menesklou and Gleiss

$$H(\phi(z,t)) = \left(1 - k\left(\frac{\phi(z,t)}{\phi_{cp}}\right)\right)^p$$

➡ Good agreement to previous works with same operational conditions

OUTLINE

TAKEI Laboratory
武居　研究室
Laboratory on Multiphase Flow and Visualization

UNIVERSITAS GADJAH MADA

- ✓ Overview of Electrical Impedance Tomography[1] (5 min)
- ✓ *In situ* measurement on industrial decanter by Wireless Electrical Resistance Tomography (WERT)[2-6] (40 min)
- ✓ **Development of Lymphedema Monitor (10 min)**
- ✓ **Concluding Remarks and Questions (5 min)**

Research Background

What is lymphedema?

- 20-30% onset after surgery for breast cancer and gynecological cancer[1-2)]
- Early detection is important for advanced chronic diseases・Significant decrease in QOL (quality of life) and ADL (activity of daily living)
- Often retreats from social life

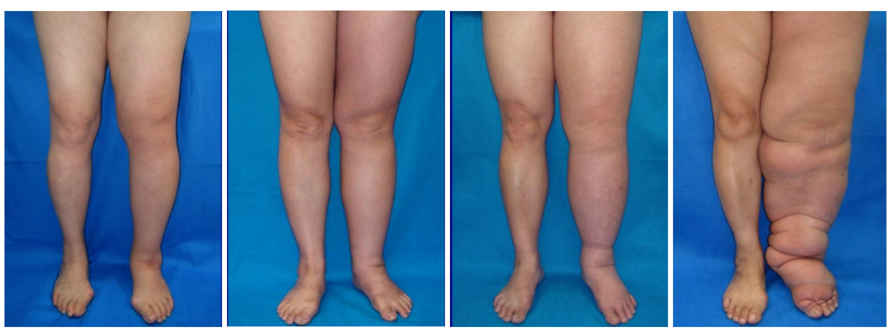

O Stages　Ⅰ Stages　Ⅱ Stages　Ⅲ Stages

Number of patients

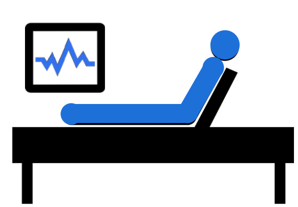

210,000 people[3)]

Increasing number of patients

6,000 people/year[3)]

[1)] Cormier JN, *Cancer* (2010)

[2)] Zou L, *Breast Cancer* (2018)

[3)] Japan Medical Lymphatic Drainage Association https://www.mlaj.jp/

Current diagnosis of lymphedema

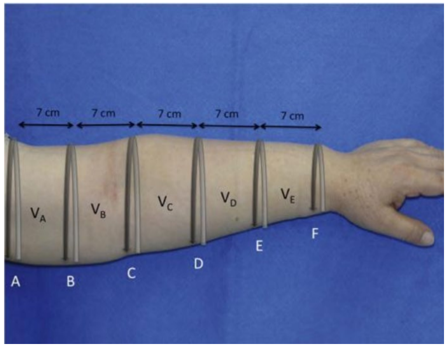

Circumferential diameter measurement [1]

Bioimpedance (BI) method [1]

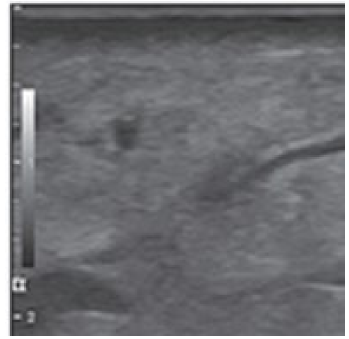

Ultrasound [2]

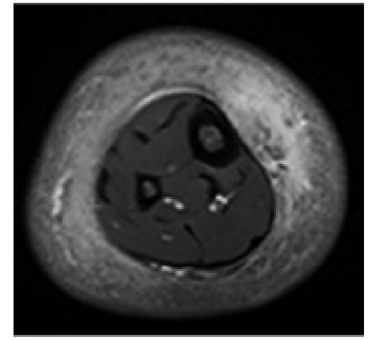

MRI [3]

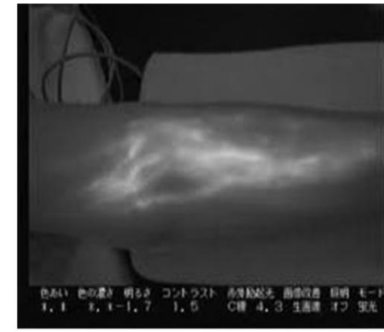

ICG 1) [1]

Lymphatic scintigraphy 2) [1]

1) Subcutaneous injection of indocyanine green (ICG) and real-time observation with near infrared rays
2) How to inject a contrast medium subcutaneously and take a picture with a gamma camera

[1] Cheng M, et al.,“Principles and practice of lymphedema surgery”, USA, Elsevier (2016)
[2] Suehiro, Kotaro, et al. "Significance of ultrasound examination of skin and subcutaneous tissue in secondary lower extremity lymphedema." Annals of vascular diseases 6.2 (2013): 180-188.
[3]Wang L, et al. Edema areas of calves measured with magnetic resonance imaging as a novel indicator for early staging of lower extremity lymphedema, Lymphat Res Biol 16, 240–247 (2018)

Development of Lymphedema Monitor

● Worries of medical staff

・ Cannot be detected early (stages 0 to I)

・ Lack of quantitatively stage detection

・ Difficult to see the effect of a lymphedema massage that relies on intuition and experience!

● Patient's worries

・I am vaguely anxious because I do not notice the initial symptoms

・I do not understand the effect of daily self-care

・I cannot share the symptoms with medical staff

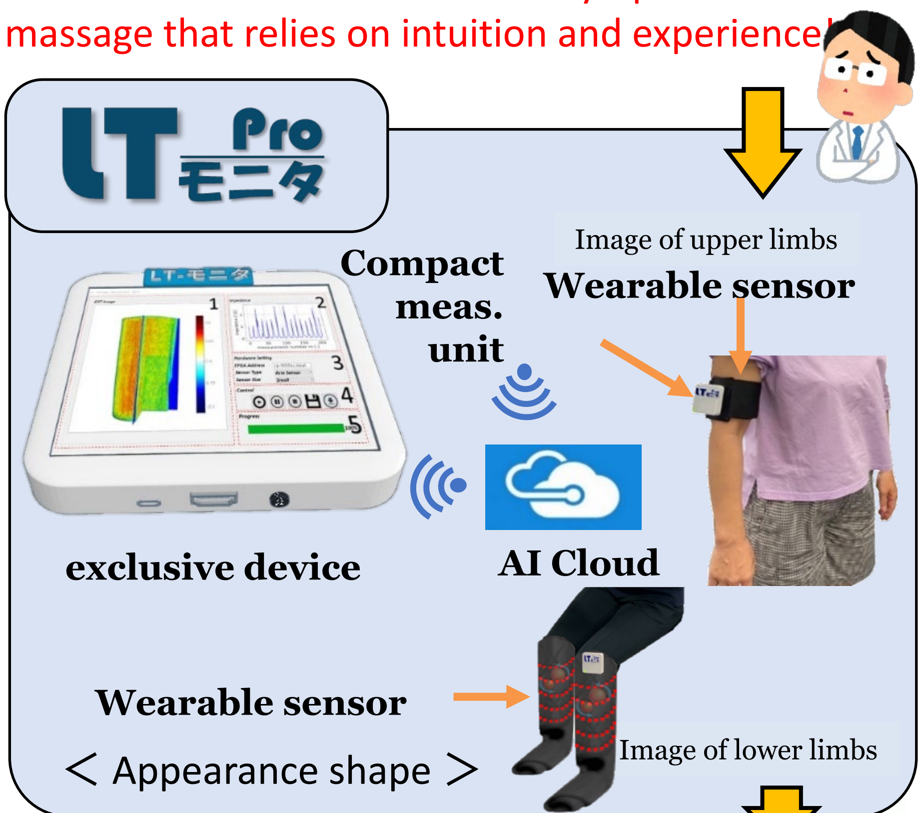

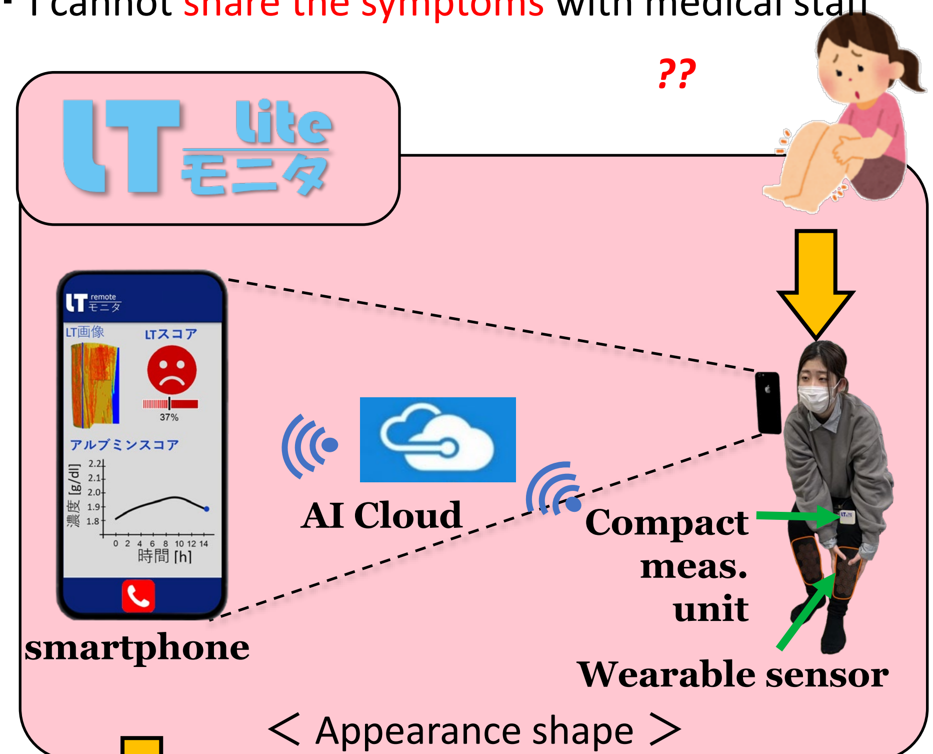

https://tenor.com/view/happy-happy-doctor-courts-courtsoptical-dr-lensman-gif-18731667

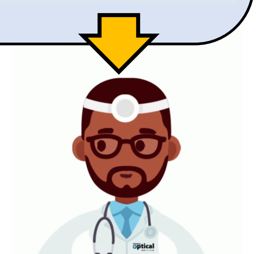

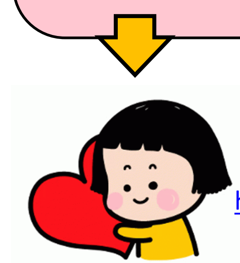

https://tenor.com/view/mobile-girl-mim-gif-21459115

OUTLINE

TAKEI Laboratory
武居　研究室
Laboratory on Multiphase Flow and Visualization

UNIVERSITAS GADJAH MADA

- ✓Overview of Electrical Impedance Tomography[1] (5 min)
- ✓ *In situ* measurement on industrial decanter by Wireless Electrical Resistance Tomography (WERT)[2-4] (15 min)
- ✓ Development of Lymphedema Monitor (5 min)
- ✓ **Concluding Remarks and Questions (5 min)**

Conclusions

- *In situ* measurement on industrial decanter is **feasible** by applying **Industrial Process Tomography**: Wireless Electrical Resistance Detector/Tomography
- **Boundary and initial condition** are important aspects to sharply develop the measurement technique
- Requirements/**focus on object's demand** is inevitable to produce an **impactful technology**

TAKEI Laboratory

武居　研究室

Laboratory on Multiphase Flow and Visualization

http://www.em.eng.chiba-u.jp/~takei/top.htm